THERMOPHYSICAL PROPERTIES MEASUREMENTS AND NUMERICAL MODELING OF NANOFLUIDS

By

Praveen Krishna Namburu

RECOMMENDED:

Chuen-Sen Lin

Debendra K Das

Advisory Committee Chair

Joon Lee

Chair, Department of Mechanical Engineering

APPROVED:

Dean, College of Engineering and Mines

Lawrence K Duffy

Dean of Graduate School

Aug 20, 2007

Date

THERMOPHYSICAL PROPERTIES MEASUREMENTS AND NUMERICAL MODELING OF NANOFLUIDS

A

THESIS

Presented to Faculty

of the University of Alaska Fairbanks

in Partial Fulfillment of the Requirements

for the Degree of

MASTER OF SCIENCE

By

Praveen Krishna Namburu, B.E

Fairbanks, Alaska

August 2007

Abstract

This thesis covers measurements of the thermophysical properties of various nanofluids containing copper oxide (CuO), silicon dioxide (SiO_2) and aluminum oxide (Al_2O_3) nanoparticles and numerical investigation on the fluid dynamic and heat transfer characteristics of nanofluids. Nanofluids are dispersions of nanometer-sized particles (<100 nm) in heat transfer liquids such as water, ethylene glycol or propylene glycol. An ethylene glycol and water (60:40 by mass) mixture was used as a base fluid in which various volume concentrations of nanofluids were dispersed. These nanofluids will be useful in the sub-arctic and arctic environments. Experiments were performed to investigate the rheological properties of CuO, SiO_2 and Al_2O_3 nanofluids. New viscosity correlations for different nanofluids as a function of volume concentration and temperature were developed. Using these correlations heat transfer performance of nanofluids as compared to the base fluid was numerically analyzed for laminar as well as for turbulent flows. Developing laminar flows in a parallel plate duct were computed for Reynolds number ranging from 100 to 2000 for various concentrations of CuO nanofluids. Turbulent convective heat transfer in circular tube geometry under a prescribed heat flux was numerically analyzed for Reynolds numbers ranging from 10^4 to 10^5. Heat transfer enhancement of various nanofluids over the base fluid was evaluated. The numerical results show enhanced heat transfer with increase in the volume concentration of nanoparticles.

Table of Contents

List of Figures

List of Tables

Acknowledgements

This document comprises my work at the Department of Mechanical Engineering at the University of Alaska Fairbanks during the years 2005-2007, and was supported by the Department of Mechanical Engineering and the Arctic Region Supercomputing Center (ARSC), for which I am very grateful. I would like to thank my principal advisor, Dr. Debendra K. Das, for the opportunity to work under his guidance. Dr. Das was instrumental in helping me in hard times and had trust and confidence in my work and skills.

I would also like to thank my advisory committee, Dr. Chuen Sen Lin and Dr. Abhijit Dandekar, for their valuable suggestions and help in completing this thesis. Special thanks to the Department of Petroleum Engineering for providing the experimental facilities to measure the viscosity of the nanofluid.

Finally, I would like to thank my family and friends for their mental support and comments about my work,

Chapter One

Introduction

1.1 Introduction of nanofluids

Nanofluids are dispersions of nanometer size (<100 nm) metallic particles (copper, aluminum, silver etc) in heat transfer liquids such as water, ethylene glycol and propylene glycol. According to Eastman et al. (2001), when 0.3 volume percent of copper nanoparticles are suspended in ethylene glycol, thermal conductivity of the fluid increases by 40%. Pak and Cho (1998) report that the convective heat transfer coefficient increases by 75% for an Al_2O_3 particle concentration of 2.78% in water. Results like these have motivated both the industrial and scientific communities to explore the heat transfer and rheological properties of nanofluids.

Determining the viscosity of the nanofluid is essential for establishing adequate pumping power as well as the convective heat transfer coefficient, as the Prandtl and Reynolds numbers (functions of viscosity) will be influenced. Until now, only a few studies have addressed the viscous properties of nanoparticle suspensions at cold temperatures. Earlier research at higher temperatures includes investigation of viscosity of carbon nanotubes (Hilding et al., 2003) and graphite nanofluids (Yang et al., 2005), $BaTiO_3$ suspensions (Tseng and Lin, 2003), nickel-terpineol suspensions (Tseng and Lin, 2003) and TiO_2 nanoparticles in water (Tseng and Lin, 2003). Results for copper oxide in ethylene glycol at room temperature (Kwak and Kim, 2005) have been presented, but no data is available for subzero temperatures. Kulkarni et al. (2007) reported that the

experimental viscosity values of Copper oxide (CuO) dispersed in propylene glycol and water mixture are much higher than those predicted by the Batchelor (1977) equation.

A great deal of energy is expended heating industrial and residential buildings in the cold regions of the world. Due to the severe winter conditions, ethylene glycol or propylene glycol mixed with water in different volume percentages are typically used to lower the aqueous freezing point of the heat transfer medium (McQuiston et al., 2000). Such heat transfer fluids are used in baseboard heaters in homes, heat exchangers, automobiles and in industrial plants in cold regions. These fluids can withstand very low temperatures. At low temperatures, ethylene glycol mixtures have better heat transfer characteristics than propylene glycol mixtures (ASHRAE, 2005). A 60% ethylene glycol and 40% water by weight fluid mixture is most commonly used in the sub-arctic and arctic regions of Alaska. We have conducted experiments with this fluid mixture by adding various nanoparticles in order to explore the thermophysical properties of such nanofluids. A thorough understanding of these properties is essential for successful application of nanofluids in cold regions.

Due to the higher magnitude of heat flux in newer microprocessor chips in electronic applications, nanofluids are an attractive option as a coolant. Presently microchannels are being considered for electronic cooling. In microchannels the Reynolds number is small due to small hydraulic diameters. Therefore, the flow may not be fully developed and is likely to be in the laminar regime. To simulate such situations, in this thesis analysis of increase in heat transfer and pressure loss of nanofluids flowing in a parallel plate duct under laminar conditions has been carefully investigated.

Using the measured rheological properties of various nanofluids, numerical analysis of turbulent forced convection was carried out, which will be useful in the design of heat transfer systems in cold climates. Comparisons of the computed Nusselt number with the correlations developed by Pak and Cho (1998) and Maiga et al. (2006) have been presented. Furthermore, the previous investigations were limited to dilute concentration up to 3 %. In the present study the Prandtl numbers are in much higher range ($47 \leq Pr \leq 105$) than those reported by the earlier researchers (Pak and Cho, 1998 and Maiga et al., 2006).

1.2 Outline of the present research

1. Determine the viscosity and rheological properties of the nanofluids with varying volume concentration of the nanoparticles. Development of new viscosity correlations that relates nanofluid viscosity with the volume concentration of dispersed nanoparticles and nanofluid operating temperature.

2. Measure the specific heat of various nanofluids and comparing with the existing theoretical correlation.

3. Numerical modeling of nanofluids incorporating the measured thermophysical properties using computational fluid dynamics code, FLUENT.

4. Numerical analysis of copper oxide nanofluid flow in a parallel plate duct was carried out. The increase in the skin friction and heat transfer with volume concentration of nanoparticles has been evaluated from simulations ranging from Reynolds number of 100 to 2000 covering the whole range of laminar regime.

5. Turbulent flow and heat transfer of three different nanofluids (CuO, Al_2O_3 and SiO_2) in an ethylene glycol and water mixture flowing through a circular tube under constant heat flux conditions has been numerically analyzed.

1.3 Summary of subsequent chapters

This thesis has been written in the manuscript format. Chapter one describes the viscosity measurements of CuO nanoparticles dispersed in EG/water. The viscosity measurements were carried out using a Brookfield viscometer. From the experimental data, a new correlation for the viscosity of nanofluids as a function of particle volume concentration and temperature was derived.

Chapter two describes the nanoparticle diameter effect on the viscosity of the nanofluids. The experiments reveal that nanofluids containing smaller diameter nanoparticles have higher viscosity. Specific heat of the nanofluids was measured and compared with the theoretical correlation. A new viscosity correlation for SiO_2 /EG water nanofluids as a function of temperature and volume concentration was derived.

Chapter three describes the numerical study for copper oxide nanofluid flow in a parallel plate duct under the laminar regime. The effects on local and average skin friction coefficients, Nusselt number and convective heat transfer coefficient have been analyzed in detail with verification of their accuracies with theoretical results. Computational results for a 10 % volume concentration CuO nanofluid shows that under laminar flow in a parallel plate duct at a Reynolds number of 2000 the heat transfer coefficient increases by 2.5 times in comparison with pure water. An adverse effect on

the wall shear stress was noticed with an increase in the volume concentration of nanofluids.

Chapter four describes the numerical study of turbulent flow and heat transfer of three different nanofluids (CuO, Al_2O_3 and SiO_2) in an ethylene glycol and water mixture flowing through a circular tube under constant heat flux conditions. All the thermophysical properties of nanofluids are temperature and volume concentration dependent. At a constant Reynolds number, Nusselt number increases by 35% for 6% CuO nanofluids over the base fluid.

1.4 References

ASHRAE Handbook Fundamentals., 2005. American Society of Heating, Refrigerating and Air-Conditioning Engineers Inc., Atlanta.

Batchelor, G.K., 1977, The effect of Brownian motion on the bulk stress in a suspension of spherical particles, Journal of Fluid Mechanics 83, 97-117.

Eastman, J.A., Choi, S.U.S., Li, S., Yu, W., Thompson, L.J., 2001. Anomalously increased effective thermal conductivities of ethylene glycol-based nanofluids containing copper nanoparticles, Applied Physics Letters 78, 718-720.

Hilding, J., Grulke, E.A., Zhang, Z.G., and Lockwood, F., 2003. Dispersion of carbon nanotubes in liquids, Journal of Dispersion Science and Technology 24, 1-41.

Kulkarni, D.P., Das, D.K., Patil, S.L., 2007. Effect of temperature on rheological properties of copper oxide nanoparticles dispersed in propylene glycol and water mixture, Journal of Nanoscience and Nanotechnology 7, 1-5.

Kwak, K., Kim, C., 2005. Viscosity and thermal conductivity of copper oxide nanofluid dispersed in ethylene glycol, Korea-Australia Rheology Journal 17, 35-40.

Maiga, S.B., Nguyen, C.T., Galanis, N., Roy., Mare, T., Coqueux, M., 2006. Heat transfer enhancement in turbulent tube flow using Al_2O_3 nanoparticle suspension, International Journal of Numerical Methods for Heat and Fluid Flow 16, 275-292.

McQuiston, F.C., Parker, J.D., Spitler, J.D., 2000. Heating Ventilating and Air conditioning, John Wiley & Sons Inc., New York.

Pak, B. C., Cho, Y. I., 1998. Hydrodynamic and heat transfer study of dispersed fluids with submicron metallic oxide particles, Experimental Heat Transfer 11, 151-170.

Tseng, W., Lin, C.L., 2003. Effect of dispersants on rheological behavior of $BaTiO_3$ powders in ethanol-isopropanol mixtures, Materials Chemistry and Physics 80, 232-238.

Tseng, W., Lin, C.L., 2003. Effect of polymeric dispersant on rheological behavior of nickel–terpineol suspensions, Material Science and Engineering A 347, 145-153.

Tseng, W., Lin, C.L., 2003. Rheology and colloidal structure of aqueous TiO_2 nanoparticle suspensions, Materials Science and Engineering A, 355 (2003)186-192.

Yang, Y., Grulke, E.A., Zhang Z.G., and Wu, G., 2005. Rheological properties of carbon nanotube and Graphite nanoparticle dispersions, Journal of Nanoscience and Nanotechnology 5, 571-579.

Chapter Two

Viscosity of Copper Oxide Nanoparticles Dispersed in Ethylene Glycol and Water Mixture

2.1 Abstract

Nanofluids are new kinds of fluids engineered by dispersing nanoparticles in base fluids. This paper presents an experimental investigation of rheological properties of copper oxide nanoparticles suspended in 60:40 (by weight) ethylene glycol and water mixture. Nanofluids of particle volume percentage ranging from 0% to 6.12% were tested. The experiments were carried over temperatures ranging from –35°C to 50°C to demonstrate their applicability in cold regions. For the particle volume concentrations tested, nanofluids exhibited newtonian behavior. An experimental correlation was developed based on the data, which relates viscosity with particle volume percent and the nanofluid temperature.

---

*Namburu, P.K, Kulkarni, D.P, Misra, D and Das, D.K.2007.Viscosity of Copper Oxide Nanoparticles dispersed in Ethylene Glycol and Water Mixture. In Press. Experimental Thermal and Fluid Science

2.2 Keywords

Nanofluid, Viscosity, Rheology, Ethylene glycol, Temperature dependency

2.3 Introduction

Nanofluids are composites consisting of solid nanoparticles with sizes varying generally from 1-100 nm dispersed in heat transfer liquids such as water, ethylene glycol, propylene glycol and so on. In the last decade, nanofluids have gained significant attention due to their enhanced thermal properties. According to Eastman et al [1], when 0.3 volume percent of copper nanoparticles are suspended in ethylene glycol, thermal conductivity of the fluid increases by 40%. Pak and Cho [2] report that the convective heat transfer coefficient increases by 75% for an Al_2O_3 particle concentration of 2.78% at a fixed Reynolds number. Results like these have motivated both the industrial and science communities to explore the heat transfer and rheological properties of nanofluids.

A great deal of energy is expended heating industrial and residential buildings in the cold regions of the world. Due to the severe winter conditions, ethylene glycol or propylene glycol mixed with water in different volume percentages are typically used to lower the aqueous freezing point of the heat transfer medium [3]. Such heat transfer fluids are used in baseboard heaters in homes, heat exchangers, automobiles and in industrial plants in cold regions. These fluids can withstand very low temperatures. At low temperatures, ethylene glycol mixtures have better heat transfer characteristics than propylene glycol mixtures [4]. A 60% ethylene glycol and 40% water by weight fluid

mixture is most commonly used in the sub-arctic and arctic regions of Alaska. We have conducted experiments with this fluid mixture by adding copper oxide nanoparticles in order to explore the thermophysical properties of such nanofluids. A thorough understanding of these properties is essential for successful application in cold regions. Xuan and Li [5] showed that a nanofluid of low concentration increases the heat transfer coefficient substantially without much penalty in pressure loss. Therefore, copper oxide nanoparticles dispersed in a glycol/water mixture in various volume percentages (0%, 1%, 2%, 3%, 4%, 5% and 6.12%) were tested to investigate the rheological characteristics of these nanofluids over temperatures ranging from -35°C to 50°C for their effective usage.

Determining the viscosity of the nanofluid is essential to establishing adequate pumping power as well as the convective heat transfer coefficient, as the Prandtl and Reynolds numbers (functions of viscosity) will be influenced. Until now, only a few studies have addressed the viscous properties of nanoparticles suspensions at cold temperatures. Earlier research at higher temperatures includes investigation of viscosity of carbon nanotubes [6] and graphite nanofluids [7], $BaTiO_3$ suspensions [8], nickel-terpineol suspensions [9], and TiO_2 nanoparticles in water [10]. Other investigations have focused on the rheology of aluminum nanoparticle suspensions in paraffin oil [11] and Al_2O_3 nanoparticles in water [12]. Results for copper oxide in ethylene glycol at room temperature [13] have been presented, but no data is available for subzero temperatures. Several available correlations for nanofluid viscosity are presented below.

Einstein [14] proposed a viscosity correlation for particle suspensions in base fluid when the volume concentration is lower than 5%.

$$\mu_s = \mu_f(1 + \frac{5}{2}\phi) \tag{1}$$

Here, μ_s = suspension viscosity, μ_f = viscosity of base fluid, and ϕ is volume percentage of particles in base fluid.

Bicerano et al [15] proposed a similar correlation which relates viscosity and volumetric suspensions by:

$$\mu_s = \mu_f(1 + \eta\phi + k_H\phi^2 + ...) \tag{2}$$

Here η is the virial coefficient and k_H is Huggins coefficient.

Brinkman [16] presented a viscosity correlation that extended Einstein's equation to concentrated suspensions.

$$\mu_s = \mu_f \frac{1}{(1-\phi)^{2.5}} \tag{3}$$

Notice that all three correlations, equations (1), (2) and (3) were developed to relate viscosity as a function of volume percentage only; there is no consideration of temperature dependence.

Generally fluids have higher viscosity near their freezing point and fairly low viscosity near their boiling temperature, showing that viscosity is a strong function of the temperature. White [17] presented a correlation for pure fluids between viscosity (μ_f) and temperature which is given by:

$$\ln \frac{\mu_f}{\mu_0} \approx a + b(\frac{T_0}{T}) + c(\frac{T_0}{T})^2 \quad (4)$$

Here (μ_0, T_0) are reference values and (a, b, c) given in the table by White, are dimensionless curve-fit constants. They vary from fluid to fluid; for example for water a = -2.10, b = -4.45 and c = 6.55. Kulkarni et al. [18] proposed a correlation that relates viscosity of copper oxide nanoparticles suspended in water and in the temperature range of 5°C to 50°C

$$\ln \mu_s = A(\frac{1}{T}) - B \quad (5)$$

Here A and B are the functions of volume percentage ϕ. As this is an aqueous solution, this correlation is not applicable for nanofluids in the subzero temperature range. Our investigation of the relation between temperature and nanofluid viscosity at subzero temperatures will help us develop the next generation of heat transfer fluids applicable in cold regions. A comprehensive review of heat transfer characteristics including viscosity measurements of nanofluids have been recently presented by Wang and Mujumdar [19].

2.4 Experimental Procedure

In our experiments, we used copper oxide nanoparticles with an average diameter of 29 nm and a particle density of 6.3 gm/cc (Nanopahse, Inc [20]). Nanofluids with different volume concentrations (2%, 4%, 6%, 8%, and 10%) were dispersed in a 60:40 (in weight) ethylene glycol and water mixture. Sample preparation was carried out using a very sensitive mass balance with an accuracy of 0.1 mg. The nanofluid mixture was

then stirred and agitated thoroughly for 30 minutes with an ultrasonic agitator similar to the preparation of nanofluids by He et al. [21]. This ensures uniform dispersion of

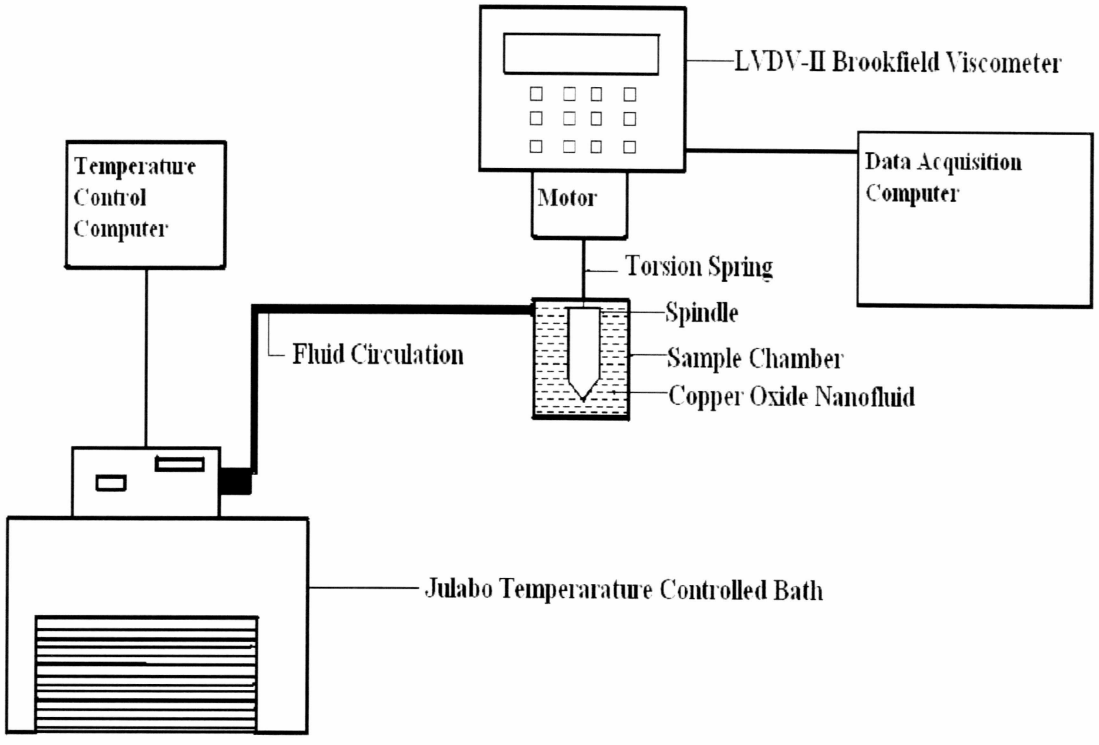

nanoparticles in the base fluid.

Figure 2.1 Experimental setup for viscosity measurement of nanofluids.

The experimental setup for the rheological property measurements of the copper oxide nanoparticles suspended in an ethylene glycol-water mixture is shown in Figure 2.1 It consists of an LV DV-II+ Brookfield programmable Viscometer [22] and Julabo temperature- controlled bath with a computer to control temperature. The viscometer drives a spindle immersed in the test fluid. When the spindle is rotated, the viscous drag

of the fluid against the spindle is measured by the deflection of the calibrated spring. This viscometer has a viscosity measurement range of 1.5 to 30,000 mPa.s and can handle the viscosity measurement results within the temperature range of this experiment. A computer controls the temperature of this bath that is used to vary the temperature of the test sample from -35°C to 50°C. Spindle SC-18 was used in this viscometer and was calibrated by using Brookfield viscosity standard fluids. The viscometer contains a sample chamber where the fluid is tested. Temperature inside the sample chamber is carefully monitored using a RTD temperature sensor during the viscosity measurements. The spindle type and speed combinations will produce satisfactory results when the applied torque is between 10-100%; therefore spindle types and speeds are selected in such a way that the torque values lie in this prescribed range. A wide range of spindle speeds are available in this viscometer (0-200 RPM).

Viscosity measurements were started at 50°C and temperature was gradually reduced to -30°C in 10° increments, with the last reading was taken at -35°C. Because the base fluid freezes at about -45°C, the experiments were carried down to a minimum temperature of -35°C with a factor of safety of 10°C.

The viscometer is connected to another computer as shown in Figure 2.1, which records the data automatically. The data collection is done by the software Wingather® [22], which collects spindle RPM, torque, viscosity, shear stress, shear rate, temperature and time. All the viscosity measurements were recorded at steady state conditions; that is, ample time (about 30 minutes) was allocated for the temperature to stabilize.

2.5 Results and Discussion

To verify the accuracy of our equipment and experimental procedure, the viscosity of the ethylene glycol and water (60:40% by weight) was measured before the addition of any copper oxide nanoparticles. The obtained readings were compared with data from the American Society of Heating, Refrigerating and Air-Conditioning Engineers (ASHRAE) handbook [4] see Figure 2.2. The ASHRAE data and the experimental values match nicely (maximum difference of ± 2%) with temperatures ranging -35°C to 50°C.

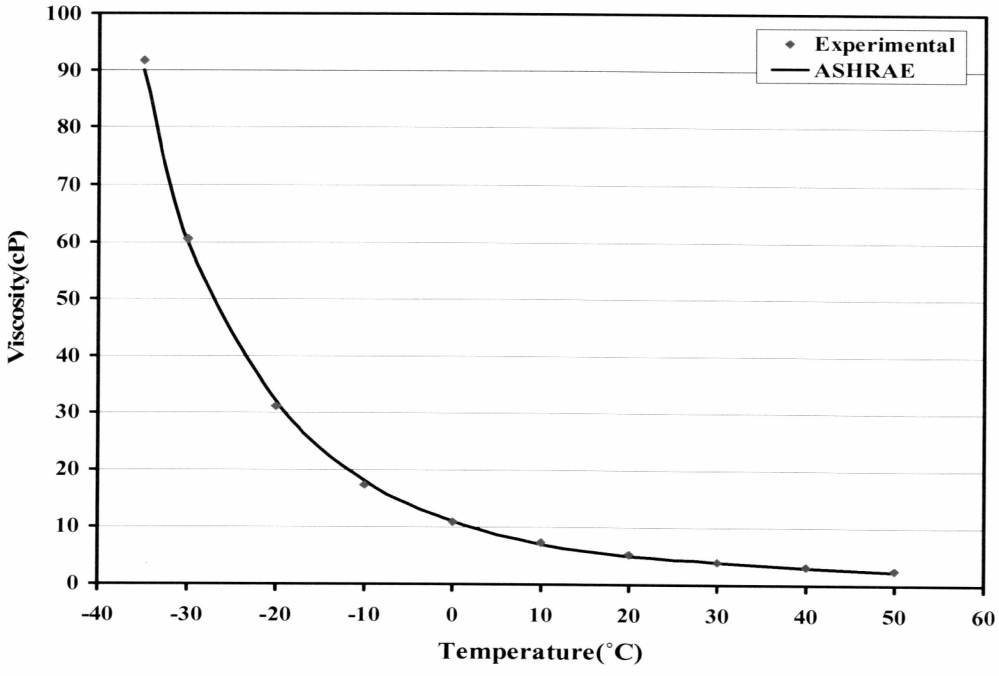

Figure 2.2 Comparison of ASHRAE viscosity values of 60:40 ethylene glycol and water mixture (by weight) and experimental data. 1 cP (centipoise) = 1 mPa.s.

The next step was to verify if the nanofluid behaves in a newtonian or non-newtonian manner. The equation governing newtonian behavior of a fluid is given by

$$\tau = \mu \dot{\gamma} \tag{6}$$

Where τ is the shear stress, μ is the coefficient of viscosity and $\dot{\gamma}$ is the shear strain rate. From the ASHRAE handbook, one observes that ethylene glycol and water mixture behaves as a newtonian fluid. While deriving the viscosity values for figure 2.2, it was found that 60:40 ethylene glycol and water at temperatures ranging from -35°C to 50°C, behaves as newtonian fluid.

The next step was to determine whether the fluid displays non-newtonian properties after the addition of copper oxide nanoparticles. Kulkarni et al. [18] observed that in experiments with copper oxide nanoparticles at volume concentrations of 5% to 15% in water, these mixtures became non-newtonian fluids in the temperature range of 5°C to 50°C. Figure 2.3 shows shear stress versus shear strain rate for 6.12% copper oxide nanoparticles concentration in ethylene glycol/water mixture at -35°C. Despite a small intercept on the shear stress axis due to measurement uncertainty, this nanofluid clearly demonstrates newtonian behavior. We believe that since ethylene glycol water mixture exhibits newtonian behavior, it dominates the rheological property and the whole mixture behaves like a Newtonian fluid with low concentrations of nanoparticles.

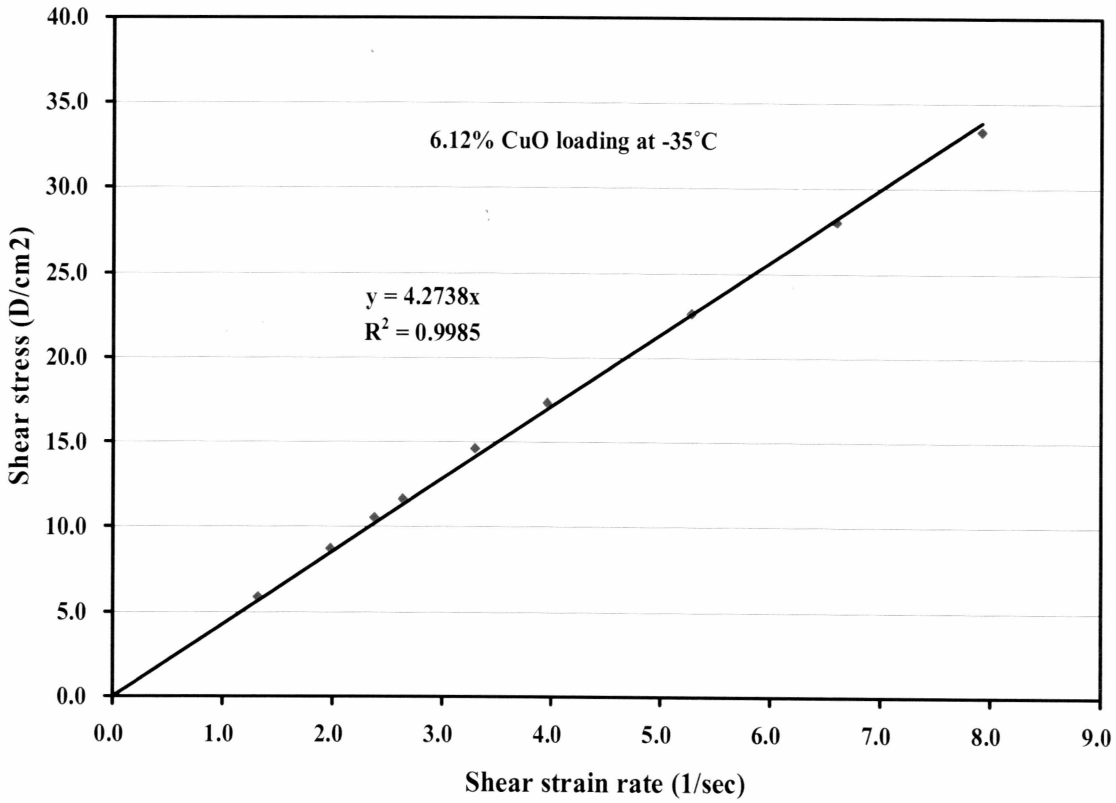

Figure 2.3 Shear stress in dyne/cm2 versus shear strain rate for 6.12% volume CuO loading at -35°C.

After we performed the base case experiments, confirming that the obtained readings were correct and that the fluid was Newtonian, viscosity measurements of fluid samples with different volume concentrations were carried out with varying temperatures between -35°C to 50°C. The results of these measurements are shown in Figure 2.4. Each data point in this plot was generated from the slope of a straight line given by the shear stress versus shear strain rate, similar to Figure 2.3. Preliminary analysis of this data indicates viscosity diminishes exponentially with a fluid temperature increase. Higher concentrations of nanofluids possess higher viscosity. The variation trends of viscosity

with temperature for all concentrations of nanofluids are similar. This indicates consistency of the trend of the experimental results.

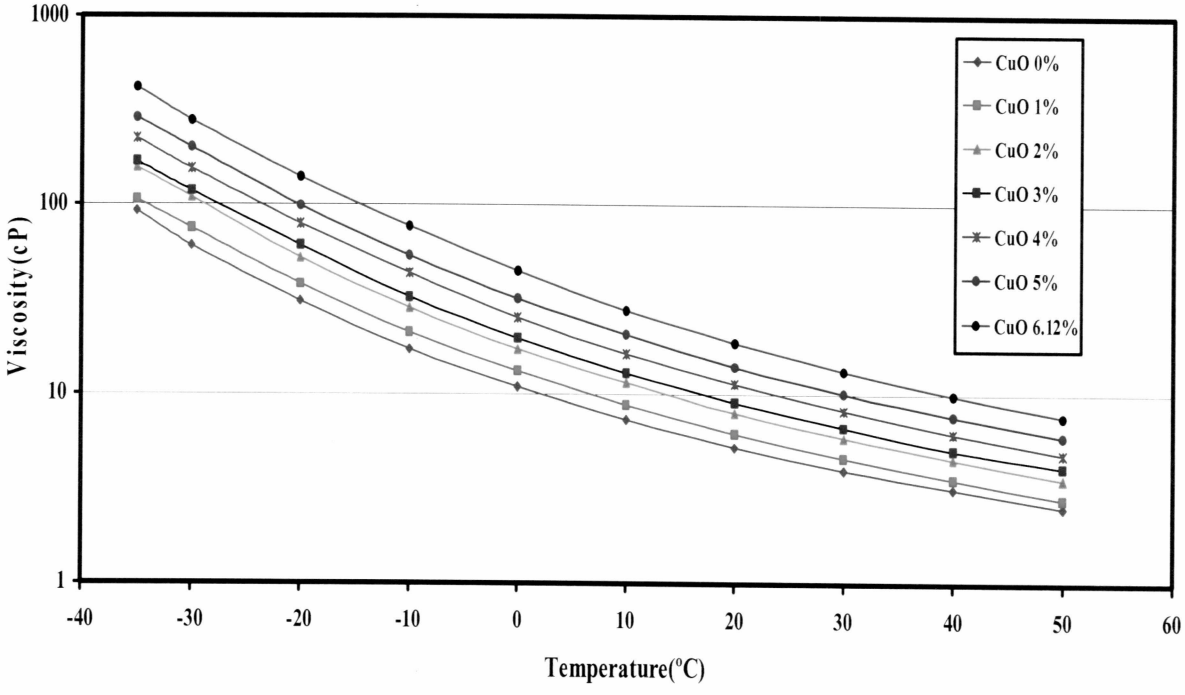

Figure 2.4 Experimental values of viscosity for various volume concentrations of nanofluids with respect to temperature.

Figure 2.5 illustrates the relationship between relative viscosity and temperature for varying volume concentrations of CuO nanoparticles in the mixture. Relative viscosity is a ratio of the viscosity of the nanofluid (μ_s) to the viscosity of the base fluid alone (μ_f). Figure 2.5 demonstrates that relative viscosity diminishes as temperature increases at a higher rate for higher concentrations of nanoparticles. At lower concentrations, the change in relative viscosity over temperature is minimal.

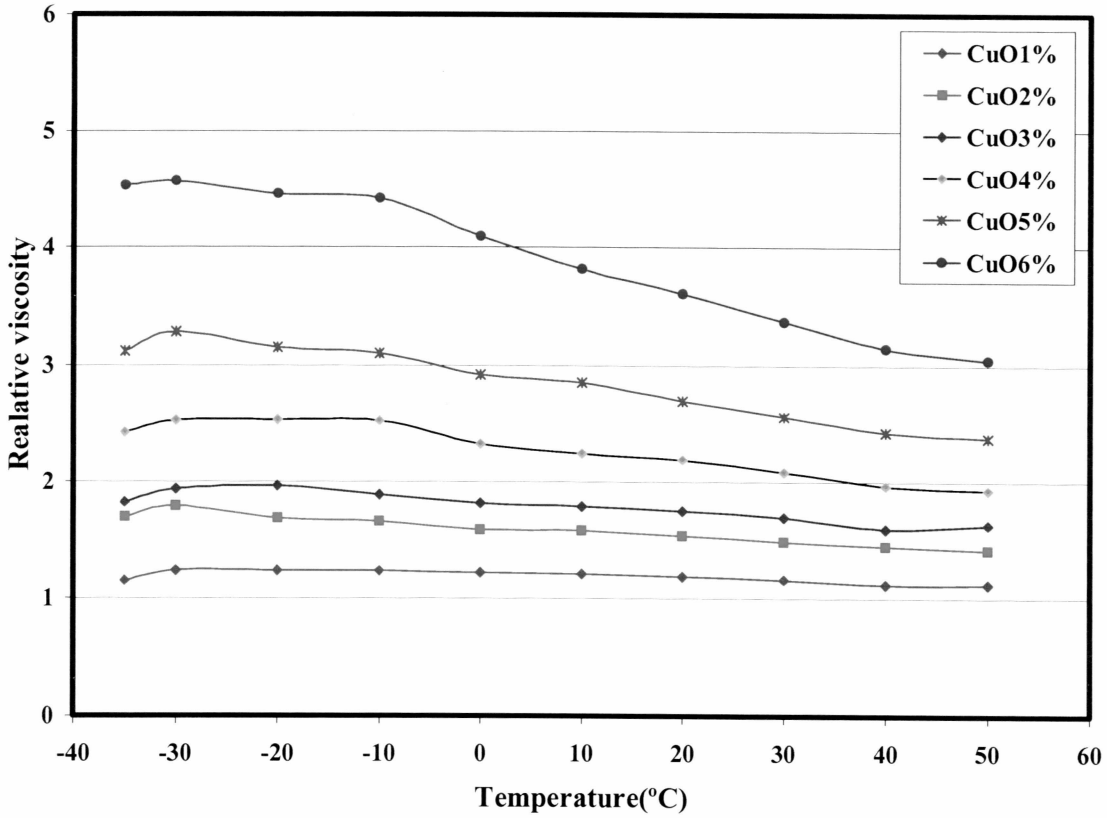

Figure 2.5 Relative viscosity and temperature relationship for various concentrations of CuO.

Different correlations were tried to fit our experimental data to correlations presented by Yaws [23], Kulkarni et al [18], Tseng [10] and White [17]. None of these correlations fit the data. Therefore, by careful statistical analyses an exponential model given by Equation (7) was derived. This equation fits the data with a correlation coefficient $R^2 > 0.99$.

$$\text{Log}\left(\mu_s\right) = Ae^{-BT} \tag{7}$$

Where μ_s is the copper oxide nanofluid viscosity in centipoise (cP), T is the temperature in K and A, B are functions of particle volume percentage (ϕ). Each volume percentage curve in Figure 4 was fitted with Equation (7) and the corresponding values of A and B were evaluated: these appear in Table 2.1 below.

Table 2.1 Curve fit values of A and B with correlation factor R2 > 0.987.

Volume Concentration (ϕ %)	0	1	2	3	4	5	6.12
A	162.76	139.27	121.77	86.22	75.27	63.02	55.32
B	0.0185	0.0177	0.0171	0.0154	0.0146	0.0137	0.0129

The coefficients A and B are related with volume concentration (ϕ) as

$$A = 1.8375(\phi)^2 - 29.643(\phi) + 165.56 \text{ with } R^2 = 0.9873 \quad (8)$$

$$B = 4 \times 10^{-6}(\phi)^2 - 0.001(\phi) + 0.0186 \text{ with } R^2 = 0.9881 \quad (9)$$

In the above expressions ϕ ranges from 0 to 6.12.

Figure 2.6 illustrates the experimental data and the curves generated using Equation (7) for viscosity versus temperature. The maximum deviation between experimental values and curve-fit values are within $\pm$ 8.8%. In Figure 6, "Exp" represents experimental values of viscosity and "CF" represents the curve-fit values from the proposed correlations.

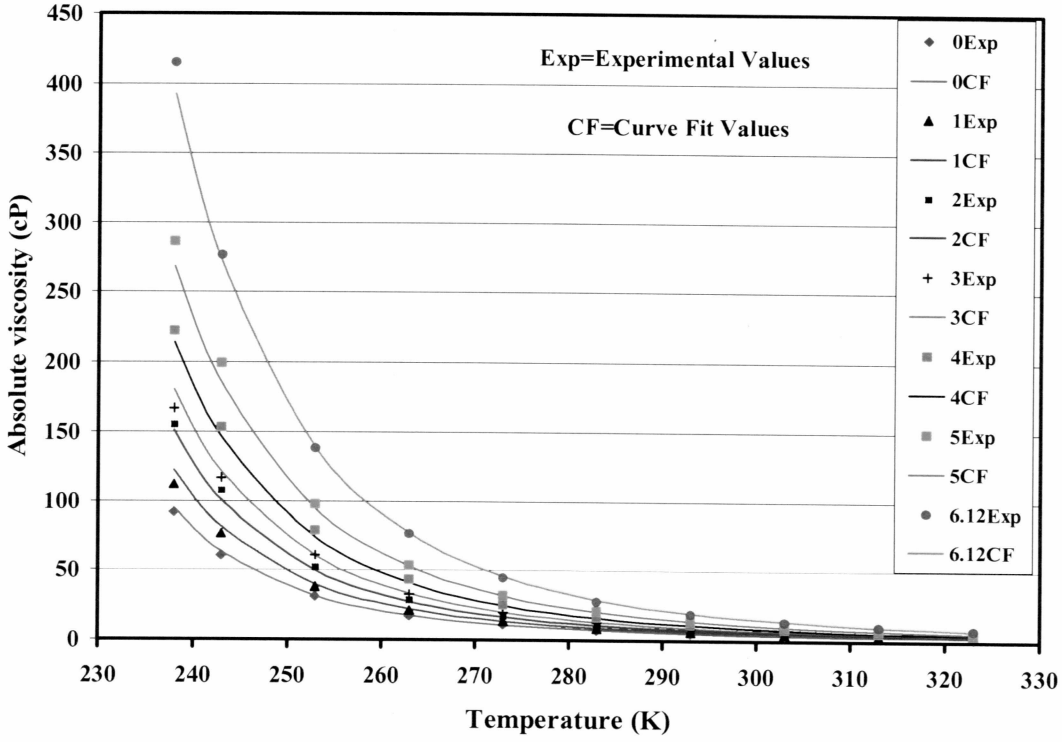

Figure 2.6 Nanofluid viscosity versus temperature of 60:40 ethylene glycol and water mixture with different volume percentage of CuO loading.

2.6 Conclusions

1. Copper oxide nanofluids exhibit Newtonian behavior in an ethylene glycol and water mixture for concentrations varying from 0 to 6.12% with temperatures ranging from -35°C to 50°C.
2. The viscosity of nanofluids increases when the volume concentration of nanoparticles increases. For example, the viscosity of 6.12% copper oxide volume concentration is about four times the value of the base fluid at -35°C.

3. As the temperature increases the viscosity of copper oxide nanofluids decreases exponentially.
4. The relative viscosity of copper oxide nanofluids is dependent on volume percentage and decreases substantially with temperature for higher concentrations.
5. A new empirical correlation expressed as Equation (7) for this nanofluid follows Arrhenius type expression where the coefficients A and B are functions of volume percentage ϕ.

2.7 Acknowledgements

Financial assistance from the Arctic Region Supercomputing Center at the University of Alaska Fairbanks is gratefully acknowledged. Authors are thankful to the Institute of Northern Engineering Petroleum Development Laboratory for providing the experimental facilities to measure viscosity.

2.8 References

[1] J.A. Eastman, S.U.S. Choi, S. Li, W. Yu and L.J. Thompson, Anomalously increased effective thermal conductivities of ethylene glycol-based nanofluids containing copper nanoparticles, Applied Physics Letters 78 (6) (2001) 718-720.

[2] B.C. Pak, Y.L. Cho, Hydrodynamics and heat transfer study of dispersed fluids with submicron metallic oxide particles, Experimental Heat Transfer 11 (1998)151-170.

[3] F.C. McQuiston, J.D. Parker, J.D. Spitler, Heating Ventilating and Air conditioning, John Wiley & Sons Inc., New York (2000).

[4] ASHRAE Handbook 1985 Fundamentals, American Society of Heating, Refrigerating and Air-Conditioning Engineers Inc., Atlanta (1985).

[5] Y. Xuan, Q. Li, Investigation on convective heat transfer and flow features of nanofluids. Journal of Heat Transfer 125 (2003) 151-155.

[6] J. Hilding, E.A. Grulke, Z.G. Zhang and F. Lockwood, Dispersion of carbon nanotubes in liquids, Journal of Dispersion Science and Technology 24 (1) (2003) 1-41.

[7] Y. Yang, E.A. Grulke, Z.G. Zhang and G. Wu, Journal of Nanoscience and Nanotechnology, 5 (2005) 571-579.

[8] W. Tseng, C.L. Lin, Effect of dispersants on rheological behavior of $BaTiO_3$ powders in ethanol-isopropanol mixtures, Materials Chemistry and Physics 80, (2003) 232-238.

[9] W. Tseng and C.N. Chen, Effect of polymeric dispersant on rheological behavior of nickel–terpineol suspensions, Material Science and Engineering A 347 (1-2) (2003) 145-153.

[10] W.J. Tseng, K.C. Lin, Rheology and colloidal structure of aqueous TiO_2 nanoparticle suspensions, Materials Science and Engineering A, 355 (2003)186-192.

[11] U. Teipel, U. Barth, Rheology of nano-scale aluminum suspensions, Propellants, Explosives, Pyrotechnics 26 (2001) 268-272.

[12] W.J Tseng, C.H. Wu, Aggregation, rheology and Electrophoretic packing structure of aqueous Al2O3 nanoparticle suspensions, Acta Materialia, 50 (2002) 3757-3766.

[13] K. Kwak, C. Kim, Viscosity and thermal conductivity of copper oxide nanofluid dispersed in ethylene glycol, Korea-Australia Rheology Journal, 17(2) (2005)35-40.

[14] A. Einstein, Investigations on the Theory of the Brownian movement, Dover Publications, New York (1956).

[15] J. Bicerano, J.F. Douglas, D.A. Brune, Model for the viscosity of particle dispersions, Journal of Macromolecular Science Review C39 (1999) 561-642.

[16] H.C. Brinkman, The viscosity of concentrated suspensions and solutions, Journal Chemistry Physics 20 (1952) 571-581.

[17] F.M.White, Viscous Fluid Flow, McGraw Hill, New York (1991).

[18] D.P. Kulkarni, D.K. Das, G. A. Chukwu, Temperature dependent rheological property of copper oxide nanoparticles suspension, Journal of Nanoscience and Nanotechnology 6 (2006) 1150-1154.

[19] X.Q. Wang, A.S Mujumdar, Heat transfer characteristics of nanofluids: a review, International Journal of Thermal Sciences 46 (2007) 1-19.

[20] Nanophase Technologies, Romeoville, IL, USA. http://www.nanophase.com.

[21] Y. He, Y. Jin, H. Chen, Y. Ding, D. Cang, H. Lu, Heat transfer and flow behavior of aqueous suspensions of TiO_2 nanoparticles (nanofluids) flowing upward through a vertical pipe, International Journal of Heat and Mass Transfer 50 (2007) 2272-2281.

[22] Brookfield DV-II+ Programmable Viscometer Manual No. M/97-164-D1000, Brookfield Engineering Laboratories Inc, Massachusetts (1999).

[23] C.L.Yaws, Physical Properties-A Guide to the Physical, Thermodynamic and Transport Property Data of Industrially Important Chemical Compounds, McGraw-Hill, New York, (1977).

Chapter Three

Experimental Investigation of Viscosity and Specific Heat of Silicon Dioxide Nanofluids

3.1 Abstract

This paper presents the results of an experimental investigation into the viscosity and specific heat of silicon dioxide (SiO_2) nanoparticles with various diameters (20 nm, 50 nm and 100 nm) suspended in a 60:40 (by weight) ethylene glycol and water mixture. Nanofluids with particle volume percentages ranging from 0% to 10% were examined. The viscosity experiments were carried out over wide temperature ranges, from –35°C to 50°C, to demonstrate their applicability in cold regions. The nanoparticle diameter effect on the rheology of the SiO_2 nanofluid is explored. Non-Newtonian behavior was observed for the particle volume concentrations of these nanofluids at sub-zero temperatures. A new correlation was developed from experimental data, which related viscosity with particle volume percent and nanofluid temperature. The specific heats of the SiO_2 nanofluids for various particle volume concentrations are presented.

---

*Namburu, P.K, Kulkarni, D.P, Dandekar, A, Das, D.K 2007. Experimental Investigation of Viscosity and Specific Heat of Silicon Dioxide Nanofluids. In Press. Micro and Nano Letters.

3.2 Keywords

Silicon Dioxide Nanoparticles; Nanofluids; Rheology; Specific Heat

3.3 Introduction

Nanofluids are composites consisting of solid nanoparticles with sizes varying generally from 1-100 nm dispersed into effective heat-transfer liquids. Water, ethylene glycol and propylene glycol are often used for many of these applications as the base fluid in nanofluids. Nanofluids are of great significance because of their enhanced thermal properties. Eastman et al [1] found, when 0.3% (volume) of copper nanoparticles was suspended in ethylene glycol, it increased the thermal conductivity of the fluid by 40%. Pak and Cho [2] reported that at a fixed Reynolds number, the convective heat transfer coefficient increased by 75% for a 2.78% (volume) Al_2O_3 nanofluid. Results like these have drawn much interest from the industrial and science communities to explore the heat transfer and rheological properties of nanofluids.

In the cold regions of the world, a great deal of energy is expended heating industrial and residential buildings. Due to severe winter conditions, ethylene glycol or propylene glycol mixed with water in different weight percentages are typically used to lower the aqueous freezing point of the heat transfer medium [3]. Such heat transfer fluids are used in home baseboard heaters, heat exchangers, automobiles and in industrial plants in cold regions. These fluids can withstand very low temperatures. At low temperatures, ethylene glycol mixtures have better heat transfer characteristics than propylene glycol mixtures [4]. A 60% ethylene glycol and 40% water by weight fluid

mixture is most commonly used in the sub-arctic and arctic regions of Alaska. We have conducted experiments with this fluid mixture containing silicon dioxide nanoparticles with average diameters of 100 nm, 50 nm, and 20 nm in various volume percentages to explore the thermophysical properties of these nanofluids. A thorough understanding of these properties is important for successful cold regions application.

Silicon dioxide nanoparticles are the least expensive nanoparticles and very little research has been done on their specific heat and rheological properties, making it an ideal test subject. Silicon dioxide nanoparticles with varying diameters were used to explore the diameter effect on the viscosity. These nanoparticles were dispersed in glycol/water mixtures with various volume percentages (2%, 4%, 6%, 8% and 10%), and then were tested to investigate the rheological characteristics with temperatures ranging from -35°C to 50°C and specific heat with temperatures ranging from 20°C to 70°C.

Determining the viscosity of the nanofluid is essential to establishing accurate pumping power, Prandtl and Reynolds numbers and the convective heat transfer coefficient. Specific heat is another important thermophysical property, since Prandtl number is also a function of specific heat. Thus far very few studies have addressed the rheological properties and specific heats of silicon dioxide nanoparticles suspensions at cold temperatures.

Viscosity values of SiO_2 nanofluids are not available in the literature, specifically at very low temperatures. Therefore these measurements are essential for successful application of nanofluids in the arctic and sub arctic climates. From experiments on SiO_2 nanofluids, fresh scientific data was gathered. From this data a new empirical correlation

for viscosity of SiO_2 nanoparticles in ethylene glycol and water as a function of temperature and particle volume concentration has been derived, which is presented as Equation (8). Another new addition to present literature is particle diameter effects on nanofluid properties, which are limited in the current literature. For the first time, the effect of particle diameter on the viscosity of SiO_2 nanofluids has been presented in this paper. It establishes the magnitude of viscosity increase with a decrease in particle diameter. Since viscosity strongly influences pressure loss, this finding has important implication in studying pumping power characteristic in nanofluid flow. The coefficients in Equations (9) and (10) fitting concentration to viscosity are quite different for other types of nanofluids, e.g., copper oxide and aluminum oxide. Comparing the viscosities of silicon dioxide with copper oxide and aluminum oxide, we notice that they are dependent on the material property of nanoparticles.

Earlier studies done at higher temperatures include investigations of the viscosity of carbon nanotubes [5], graphite nanofluids [6], $BaTiO_3$ suspensions [7], nickel-terpineol suspensions [8], and TiO_2 nanoparticles in water [9]. Other investigations focused on the rheology of aluminum nanoparticle suspensions in paraffin oil [10] and Al_2O_3 nanoparticles in water [11]. Earlier research results for copper oxide in ethylene glycol at room temperature [12] have been presented, but no data is available for subzero temperatures. Several available correlations for nanofluid viscosity are summarized below.

Einstein [13] proposed a viscosity correlation for particle suspensions in base fluid, which is given by:

$$\mu_s = \mu_f(1+\frac{5}{2}\phi) \tag{1}$$

Where, μ_s = suspension viscosity, μ_f = viscosity of base fluid, and ϕ is volume percentage of nanoparticles in a base fluid.

Bicerano et al. [14] proposed a similar correlation which relates viscosity and volumetric suspensions by:

$$\mu_s = \mu_f(1+\eta\phi+k_H\phi^2+.....) \tag{2}$$

Here, η is the virial coefficient, and k_H is Huggins coefficient.

Brinkman [15] presented a viscosity correlation that relates viscosity and volume percentage of nanoparticles given by:

$$\mu_s = \mu_f \frac{1}{(1-\phi)^{2.5}} \tag{3}$$

Notice that all three correlations, equations (1), (2) and (3) were developed to relate viscosity as a function of volume percentage only; there is no consideration of temperature dependence. In the present paper, we have developed a temperature depended correlation for the viscosity of silicon dioxide nanofluids

Generally fluids have higher viscosity near their freezing point and fairly low viscosity near their boiling temperature, this demonstrates that viscosity is a strong function of the temperature. White [16] presented a correlation for pure liquids between viscosity and temperature which is given by:

$$\ln\frac{\mu}{\mu_0} \approx a+b(\frac{T_0}{T})+c(\frac{T_0}{T})^2 \tag{4}$$

Here (μ_0, T_0) are reference values and (a, b, c) are dimensionless curve-fit values. Kulkarni et al. [17] proposed a correlation that relates viscosity of copper oxide nanoparticles suspended in water at temperatures ranging from 5°C to 50°C.

$$\ln \mu_s = A(\frac{1}{T}) - B \tag{5}$$

Here A and B are the functions of volume percentage ϕ. As this is an aqueous solution, this correlation is not applicable for nanofluids in the subzero temperature range. Our investigation of the relation between temperature and nanofluid viscosity at subzero temperatures will help us develop the next generation of heat transfer fluids applicable in cold regions.

3.4 Experimental Setup for Viscosity Measurement

In our experiments, we used silicon dioxide nanoparticles with average diameters of 20 nm, 50 nm, 100 nm and a particle density of 2.33 gm/cc (Nanophase, Inc [18]). The particles were spherical in shape, they were non porous single crystals and chemically pure. The particles were well dispersed initially and they did not aggregate or settle over more than one year since we performed our experiments. The base fluid used was ethylene glycol and water mixture, 60:40 by weight. To this base fluid SiO_2 nanoparticles were added to make nanofluids of different volume concentrations of 2%, 4%, 6%, 8% and 10%. Sample preparation was carried out using a very sensitive mass balance with an accuracy of 0.1 mg.

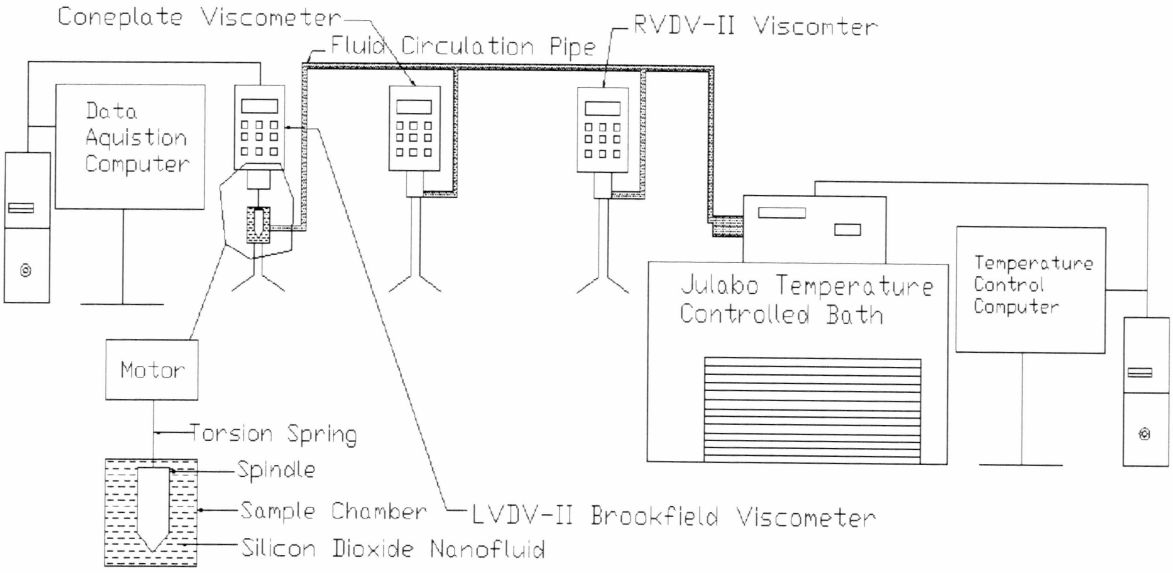

Figure 3.1 Experimental setup for viscosity measurement of silicon dioxide nanofluids.

The experimental setup for the rheological property measurements of the silicon dioxide nanoparticles suspended in an ethylene glycol-water mixture is shown in Figure 3.1. It consists of an LV DV-II+ Brookfield programmable Viscometer [19] and a Julabo temperature controlled bath connected to a computer to control the temperature. The viscometer drives a spindle immersed in the test fluid. As the spindle is rotated, the viscous drag of the fluid against the spindle is measured by the deflection of the calibrated spring. This viscometer has a viscosity measurement range of 1.5 to 30,000 mPa.s and can handle the viscosity measurement results within a temperature range of -35°C to 80°C. Since sub-arctic region usage of nanofluids will have temperatures in the lower range, where viscosity changes drastically, we focused on property measurement at

the low range. It was observed that the change in viscosity is small between 50°C and 80°C. Therefore we have conducted the experiments at temperatures ranging from -35°C to 50°C. A computer controls the temperature of the bath to vary the temperature of the test sample from -35°C to 50°C. A SC4-18 spindle was used in this viscometer and was calibrated by using Brookfield silicon viscosity standard fluids. The viscometer contains a sample chamber where the fluid is tested. Temperature inside the sample chamber is carefully monitored using a RTD temperature sensor during the viscosity measurements. The spindle type and speed combinations will produce satisfactory results when the applied torque is between 10-100% of the maximum permissible torque. Spindle types and speeds are selected in such a way that the torque values lie in this prescribed range. A wide range of spindle speeds are available in this viscometer (0-200 RPM).

Viscosity measurements started at 50°C and temperature was gradually reduced to -30°C in 10°C decrements, with the last reading was taken at -35°C. Because the base fluid freezes at about -45°C, the experiments were carried down to a minimum temperature of -35°C with a factor of safety.

The viscometer is connected to another computer as shown in Figure 3.1, which automatically records the data. The data collection is done by Wingather® software, which collects spindle RPM, torque, viscosity, shear stress, shear rate, temperature and time. All the viscosity measurements were recorded at steady state conditions; that is, ample time (about 30 minutes) was allocated for the temperature to stabilize.

3.5 Discussion of Viscosity Results

For verifying the accuracy of our equipment and experimental procedure, the viscosity of the ethylene glycol and water (60:40 by weight) was measured before the addition of any silicon dioxide nanoparticles. The obtained readings were compared with data from the American Society of Heating, Refrigerating and Air-Conditioning Engineers (ASHRAE) handbook [4]. The ASHRAE data and the experimental values matched closely (maximum difference of ± 2%) with temperatures ranging from -35°C to 50°C.

Prior studies e.g. Kulkarni et al. [17] showed that adding nanoparticles changed the behavior of the base fluid to non-Newtonian. Therefore, one objective of our experiment was to verify if the nanofluid behaved in a Newtonian or a non-Newtonian manner. The equation that governs Newtonian behavior of a fluid is given by

$$\tau = \mu \dot{\gamma} \tag{6}$$

Where, τ is the shear stress, μ is the coefficient of viscosity and $\dot{\gamma}$ is the shear strain rate. ASHRAE handbook [4] shows that ethylene glycol and water mixtures behave as Newtonian fluids. While measuring the viscosity values, it was observed that a 60:40 ethylene glycol and water mixture behaved as a Newtonian fluid between the temperature of -35°C to 50°C.

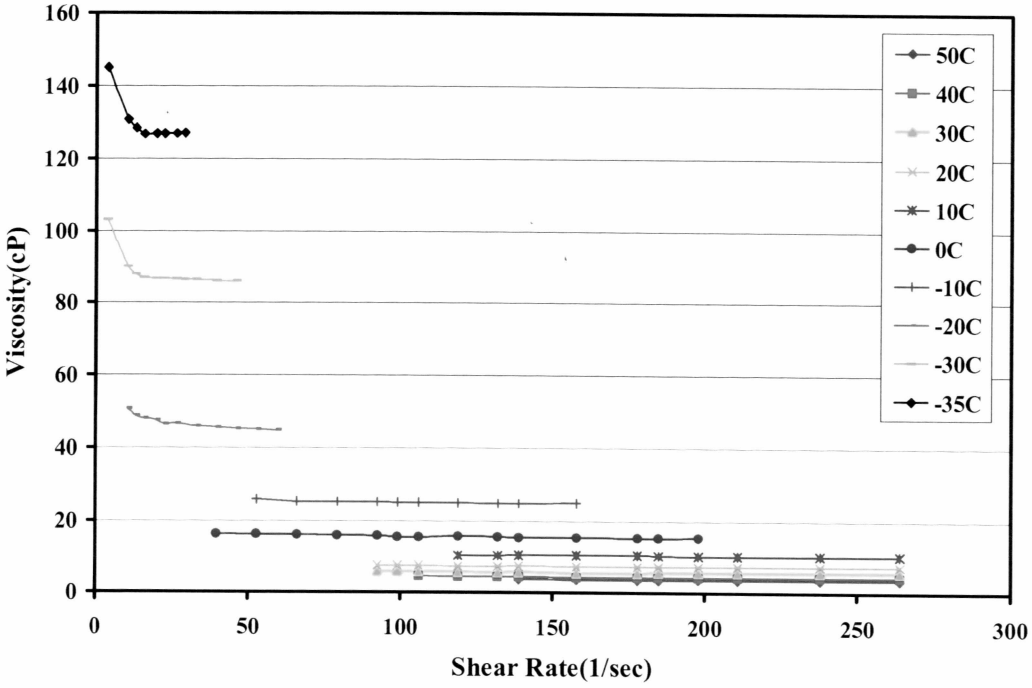

Figure 3.2 Viscosity of the silicon dioxide nanofluid (50 nm) with 6% volume concentration versus shear rate for varying temperatures from 50°C to -35°C.

Figure 3.2 illustrates viscosity versus shear rate for 6% of 50nm silicon dioxide nanoparticles in ethylene glycol and water. The curves between viscosity and shear rate are horizontal straight lines for temperatures more than -10°C; this clearly demonstrates that silicon dioxide nanofluids display Newtonian behavior. For the temperatures below -10°C, the nanofluids demonstrate non-Newtonian behavior as the curves are nonlinear and the viscosity varies with shear rate.

After performing the bench mark test case experiments and examining the behavior of the silicon dioxide nanofluids at lower temperatures, viscosity measurements

were carried out for silicon dioxide nanofluids with various diameters (20 nm, 50 nm, 100 nm) and with varying particle volume concentrations (2%, 4%, 6%, 8% and 10%) between temperatures of -35°C to 50°C.

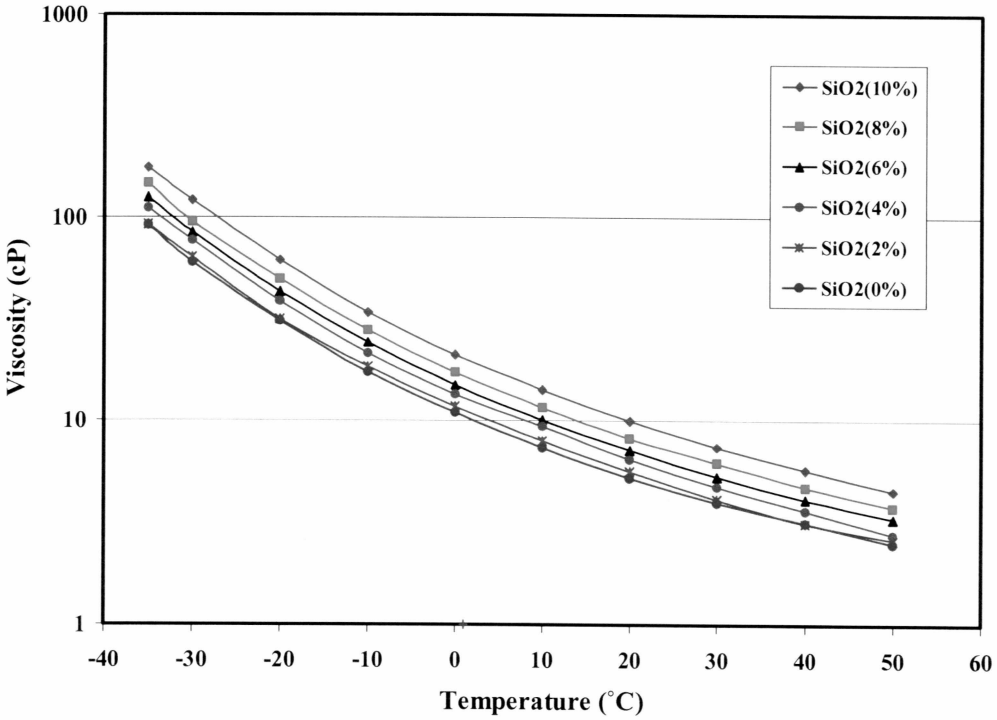

Figure 3.3. Experimental values of viscosity for varying volume concentrations of silicon dioxide nanofluids (50 nm) with respect to temperature.

Figure 3.3 is a semi-log plot of viscosity versus temperature. Data analysis of this figure indicates that viscosity diminishes exponentially as the sample fluid temperature increases. Furthermore, it shows that with higher nanoparticle concentrations, nanofluids possess higher viscosity. The shape of each curve for different concentrations of

nanofluids in Figure 3.3 is similar, which indicates consistency of trend of the experimental measurements. Similar trends were observed for viscosity measurements of silicon dioxide nanofluids with nanoparticle diameters of 20 nm and 100 nm.

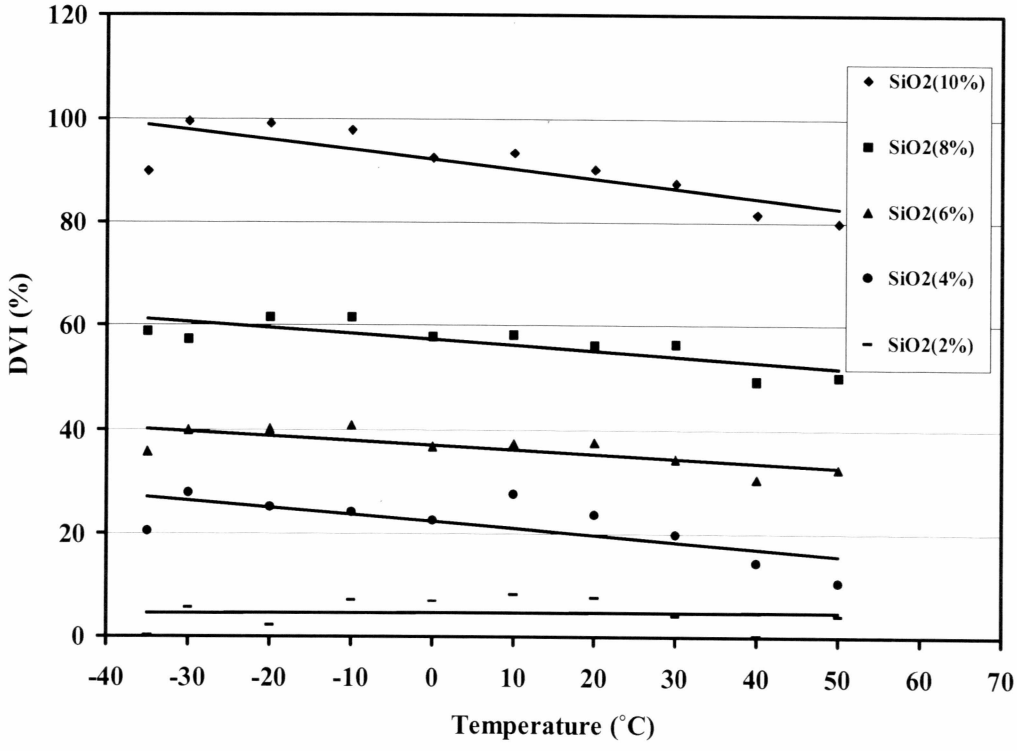

Figure 3.4. Degree of viscosity increase versus temperature for varying concentrations of silicon dioxide nanofluids (50 nm).

Figure 3.4 displays the degree of viscosity increase (DVI) versus the temperature for varying concentrations of silicon dioxide nanoparticles in ethylene glycol and water. The DVI is defined as the ratio the between difference of nanoparticles suspension viscosity μ_s and the viscosity of base fluid μ_f to the viscosity of base fluid.

Degree of viscosity increase (DVI) = $(\mu_s - \mu_f)/ \mu_f$ (7)

From the Figure 4, we infer that the DVI reduces from -35°C to 50°C for all nanofluid concentrations. If the concentration of nanoparticles is low, the DVI will be low as well. With 2% nanofluid volume concentration, the DVI is about 5%, whereas a 10% volume concentration, the DVI is about 90%.

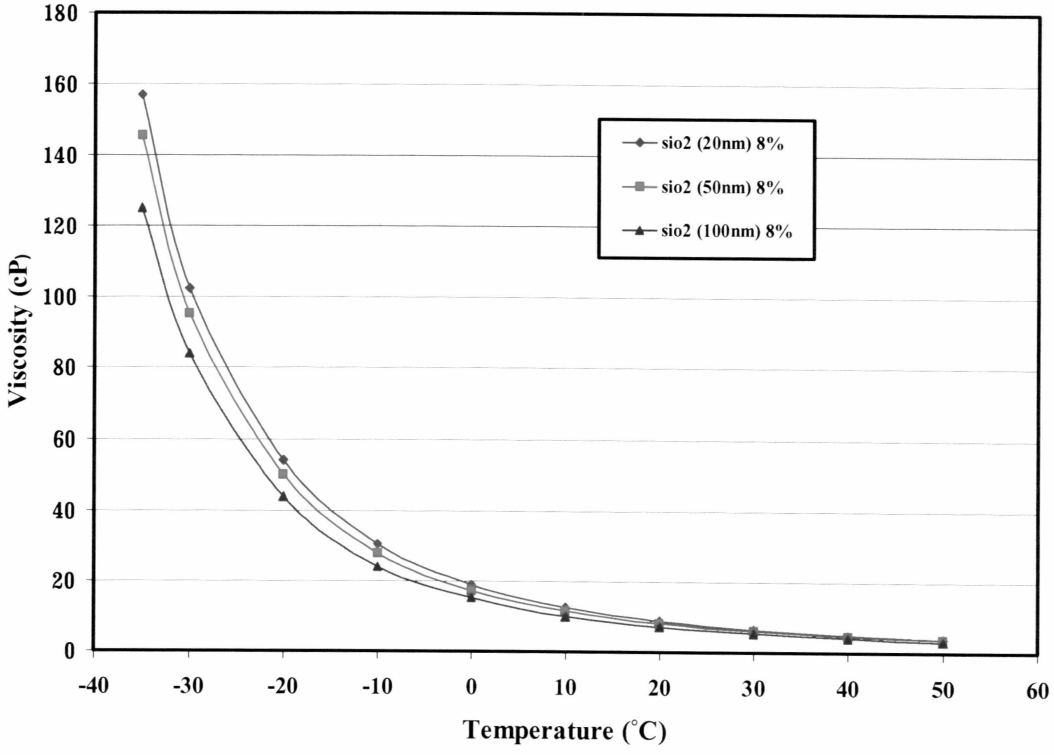

Figure 3.5 Effect of silicon dioxide nanoparticle diameter on nanofluid viscosity for varying temperature.

From Figure 3.5, we infer that for the same volumetric concentration of 8%, silicon dioxide nanofluids with highest nanoparticle diameter 100 nm have the lowest viscosity. This observation is consistent with that presented by Cheremisinoff [20] for micro particles. Similar trends of experimental results were obtained for all concentrations of silicon dioxide nanofluids.

A careful statistical analysis of experimental data revealed an exponential correlation given by Equation (8), which fits the data with a correlation factor $R^2 > 0.99$.

$$Log\ (\mu_s) = Ae^{-BT} \tag{8}$$

Here (μ_s) is the silicon dioxide nanofluid viscosity in centipoise (cP), T is the temperature in Kelvin and A and B are the functions of particle volume concentration (ϕ). Each volume percentage curve in Figure 3.6 was fitted with Equation (8) and corresponding values of A and B were evaluated, which are tabulated below.

Table 3.1 Curve fit values of A and B with correlation factor $R^2 > 0.99$.

Volume concentration (ϕ)	10%	8%	6%	4%	2%
A	69.97	91.43	103.13	139.56	154.77
B	0.0145	0.0157	0.0164	0.0177	0.0183

The coefficients A and B are related to volume percentage given by:

$$A = 0.1193\,(\phi)^{3} - 1.9289\,(\phi)^{2} - 2.245\,(\phi) + 167.17 \text{ with } R^2 = 0.981 \quad (9)$$

$$B = -7E^{-6}\,(\phi)^{2} - 0.0004\,(\phi) + 0.0192 \text{ with } R^2 = 0.99 \quad (10)$$

In the above expression, ϕ ranges from 2 to 10.

Equation (8) follows a logarithmic expression presented for viscosities of many liquids by Yaws [21]. The experimental values are within ± 8.4% with the curve fit values.

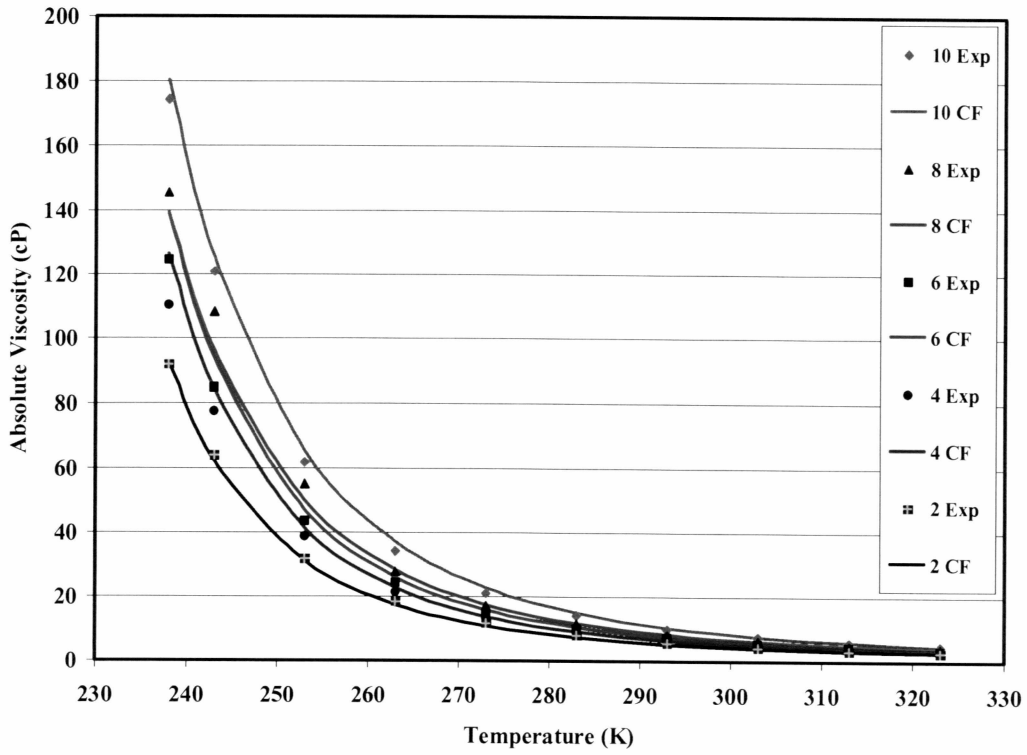

Figure 3.6 Experimental values and curve fit (CF) values of absolute viscosity versus temperature for 60:40 ethylene glycol and water with different volume percentages of silicon dioxide (50 nm).

3.6 Specific Heat Measurement

The experimental setup for measuring specific heat of silicon dioxide nanoparticles dispersed in ethylene glycol and water consists of a container in which silicon nanofluids are heated to higher temperatures by using an electrical heating element. Four copper-constantan thermocouples are placed at equal distances from the heating element to monitor the temperature increase of the silicon dioxide nanofluids. These thermocouples are attached to a data logger, which is programmed to record the temperature data in 5-second intervals. The container is well insulated to eliminate the heat transfer to the surroundings. A variac is used to supply constant power to the heating element, which is monitored by a power meter.

The specific heat of pure water was measured to verify the accuracy of the specific heat measuring equipment and the experimental procedure. Water of mass 1.3 kg was used in the container for the specific heat measurement. A constant power of 40 watts was supplied to the heating element to increase the temperature of water. The temperature change was recorded every five seconds using the data logger. Specific heat of the water was calculated from:

$$Q = m\,(Cp)\,\Delta T \tag{11}$$

Here, Q is the heat energy input in joule, m is the mass of the water (kg), Cp is the specific heat of the water (J/kg-K) and ΔT is the temperature differential (K). From the slope of a straight line from Q versus $m\Delta T$ plot, the specific heat of water was determined. The experimental value of specific heat 4189.8 J/kg.K differed by ± 0.2%, when compared with the ASHRAE [4] value of 4182 J/kg.K.

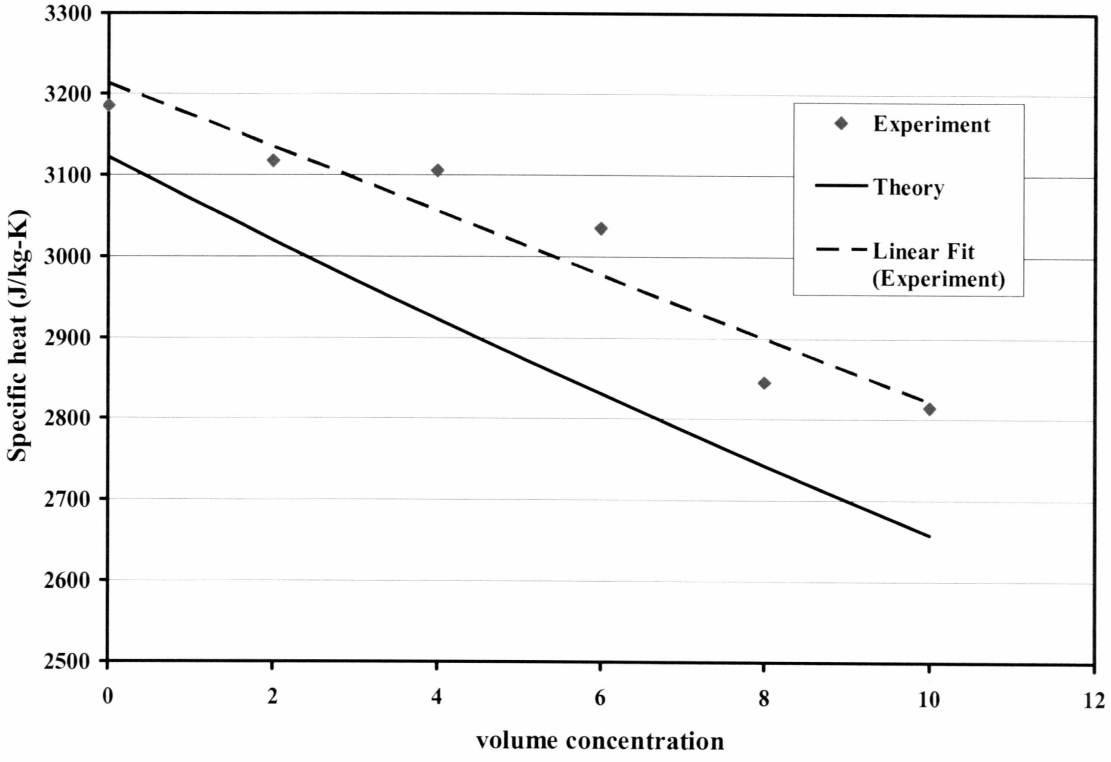

Figure 3.7 Experimental values of specific heat for silicon dioxide nanofluids (20 nm) in various concentrations suspended in ethylene glycol and water solution.

Figure 3.7 displays the variation of specific heat from experiment and theory for varying concentrations of the silicon dioxide nanofluids. The experimental values are compared with the theoretical relation presented in Buongiorno [22]. As the particle volume concentration increases, the specific heat of the silicon dioxide nanofluid decreases, which implies that for higher concentrations of silicon dioxide nanofluid, less heat input is required to increase the temperature of the nanofluid. The linear curve-fit to

the experimental data presented in Figure 7 differs from the theoretical relation of Buongiorno equation by an average deviation of 4.5%.

3.7 Conclusions

Silicon dioxide nanofluids with ethylene glycol/water as base fluids exhibit non-Newtonian behavior at lower temperatures. At higher fluid temperatures, the viscosity and shear rate relation do not change, proving Newtonian behavior. The viscosity of SiO_2 nanofluids increases as volumetric nanoparticle concentration increases. For example, the viscosity of 10% SiO_2 particle volume concentration is about 1.8 times the viscosity of the base fluid. As temperature increases, the viscosity of SiO_2 nanofluid decreases exponentially. For SiO_2 nanofluids, there is a 5% increase in DVI over the base fluid with a 2% particle volume concentration. The DVI modestly decreases as the fluid temperature increases. For the same particle volume concentration, as the particle diameter increases the viscosity of SiO_2 nanofluids decreases. A new empirical correlation between the viscosity, nanoparticle volume concentration and temperature of SiO_2 nanofluid has been derived in Equation (8). The maximum deviation between the curve-fit equation value and the experimental data is ± 8.4% with a correlation factor greater than 0.99. The specific heat of SiO_2 nanofluid decreases as nanoparticle volume concentration increases. With a 10% SiO_2 nanoparticle concentration, the specific heat is about 12% lower than that of the base fluid.

3.8 References

[1] J.A. Eastman, S.U.S. Choi, S. Li, W. Yu and L.J. Thompson, Appl. Phys. Lett., 78:6, (2001) 718-720.

[2] B.C. Pak, Y.L. Cho, Exp Heat Transfer, 11, (1998)151-170.

[3] F.C., McQuiston, J. D. Parker, J. D., Spitler, Heating, Ventilating, and Air Conditioning, John Wiley & Sons Inc., New York (2000).

[4] ASHRAE Handbook 1985 Fundamentals, American Society of Heating, Refrigerating and Air-Conditioning Engineers Inc., Atlanta (1985).

[5] J. Hilding, E.A. Grulke, Z.G. Zhang and F. Lockwood, J. Dispersion Sci. and Tech. 24:1, 1 (2003) 1-41.

[6] Y. Yang, E.A. Grulke, Z.G. Zhang and G. Wu, J. Nanosci. Nanotechnol. 5, (2005) 571 -579.

[7] W. Tseng and C.L. Lin, Mater. Chem. and Phys. 80, (2003) 232-238.

[8] W. Tseng and C.N. Chen, Mater. Sci. Eng., A347, (2003) 145-153.

[9] W.J. Tseng and K.C. Lin, Mater. Sci. Eng., A355, (2003) 186-192.

[10] U. Teipel, U. Forter-Barth, Propellants, Explosives, Pyrotechnics, 26, (2001) 268-272.

[11] W. Tseng and C.H. Wu, Acta Materialia, 50, (2002) 3757-3766.

[12] K. Kwak, C. Kim, Korea-Australia Rheology J., 17:2, (2005) 35-40.

[13] A. Einstein, Investigations on the Theory of the Brownian Movement, Dover, New York (1906).

[14] J. Bicerano, J.F. Douglas, D.A. Brune, J. Macromolecular Sci. Rev., C39:4, (1999) 561-642.

[15] H.C. Brinkman, The viscosity of concentrated suspensions and solutions, Journal Chemistry Physics 20 (1952) 571-581.

[16] F.M.White, Viscous Fluid Flow, McGraw Hill, New York (1991).

[17] D.P. Kulkarni, D.K., Das, G. A. Chukwu, J. Nanosci. and Nanotechnol., 6, (2006) 1150-1154.

[18] Nanophase Technologies, Romeoville, IL, USA. http://www.nanophase.com

[19] Brookfield DV-II+ Programmable Viscometer Manual No. M/97-164-D1000, Brookfield Engineering Laboratories Inc, MA, USA (2000).

[20] Cheremisinoff, N.P., Encyclopedia of Fluid Mechanics, Rheology and Non Newtonian Flows, vol. 7, Golf Publishing Company, Houston (1988).

[21] C.L.Yaws, Physical Properties-A Guide to the Physical, Thermodynamic and Transport Property Data of Industrially Important Chemical Compounds, McGraw-Hill, New York, (1977).

[22] J.Buongiorno, ASME J. of Heat Transfer, 128. (2006) 240-250.

Chapter Four

Numerical Study of Heat Transfer and Fluid Flow of CuO Nanofluids in a Parallel Plate Duct Under Laminar Regime

4.1 Abstract

A numerical study for copper oxide nanofluid flow in a parallel plate duct has been presented under laminar regime. The effects on local and average skin friction coefficients, Nusselt number and convective heat transfer coefficient have been analyzed in detail with verification of their accuracies with theoretical results. The increase in the skin friction and heat transfer with volume concentration of nanoparticles has been evaluated from simulations ranging from Reynolds number of 100 to 2000. The geometry was selected to simulate analysis of simultaneous hydrodynamic and thermally developing flows. Computational results for a 10% volume concentration CuO nanofluid shows that under laminar flow in parallel plate duct at a Reynolds number of 2000 the heat transfer coefficient increases by 2.5 times in comparison with pure water. From a detailed analysis summarized in a table, it is observed that there is a steeper increase in pressure loss with concentration. From similar analysis judicious decisions can be made to select various percentage concentrations of nanofluids while balancing the heat transfer requirement with the pumping power cost.

---

*Namburu, P. K. and Das, D K. 2007. Numerical Study of Heat Transfer and Fluid Flow of CuO Nanofluids in a Parallel Plate Duct Under Laminar Regime. In Review. Applied Thermal Engineering.

4.2 Keywords

Nanofluid; Laminar flow; Heat transfer enhancement; Copper oxide nanoparticles; Electronic cooling;

4.3 Introduction

Nanofluids have attained a great deal of attention in recent years as promising heat transfer fluids, suspension of metallic nanoparticles generally less than 100 nm in diameter in a base fluid constitutes a nanofluid. Because of higher thermal conductivity of nanofluids in comparison to a base fluid, higher convective heat transfer coefficients are achieved. Therefore, research is underway to apply nanofluids in environments where higher heat flux is encountered and the base fluid is not capable of achieving the desired heat transfer rate.

Due to the higher magnitude of heat flux in newer microprocessor chips in electronic applications, nanofluids are an attractive option as coolant. Presently microchannels are being considered for electronic cooling. In microchannels the Reynolds number is small due to small hydraulic diameters. Therefore, the flow may not be fully developed. In this paper we have focused on computing heat transfer and pressure loss in developing flow fields of a nanofluid of varying volumetric concentration in a parallel plate duct to evaluate their performance.

Pak & Cho [1] performed viscosity, pressure loss and heat transfer measurements on titanium dioxide nanofluids up to 3% concentration by volume and found single-phase correlations can be successfully extended to nanofluids. Xuan and Li [2] performed experimental study on Cu-water nanofluids up to 2% volume concentration and

developed a Nusselt number correlation. They found that Cu-water dilute nanofluids have almost same pressure loss as water under the same Reynolds number. Yang et al. [3] presented laminar heat transfer results with graphite nanoparticles of 2% by weight and compared Gratez number variation with Nusselt number with their experimental data and single-phase laminar flow correlation. Buongiorno [4] have considered several slip mechanisms and have proposed a correlation for the Nusselt number stressing the effect of thermophoresis.

Akbarinia and Behzadmehr [5] presented a numerical study of nanofluids under mixed laminar convection in a curved tube. They compared the variations of Nusselt number with Grashof number for various volume percentages of Al_2O_3 nanoparticles in water. They found that at large Grashof number the skin friction was reduced. Maiga et al. [6] studied γ - Al_2O_3 nanofluids flow under forced laminar convection in circular tubes and between parallel disks. For a range of Reynolds number from 250 to 1000 they concluded that the heat transfer enhancement is much more pronounced with the increase in particle concentration. However, they observed a drastic adverse effect on wall shear stress in comparison to the base fluid. For the analysis of flow between discs, they found insignificant effect on heat transfer with the variation of gap between the discs. Behzadmehr et al. [7] simulated turbulent forced convection of 1% volume concentration of Cu nanofluids in a circular tube with uniform heat flux. Their results showed Nusselt number enhancement with Reynolds number in the axial direction. They also showed that skin friction variation in the axial direction was close between water and 1% volume concentration of Cu nanofluid.

4.4 Development of model

The computational domain considered in the present analysis is a rectangular channel with length (L) = 100 mm and height (H) = 15 mm as shown in Figure 4.1.

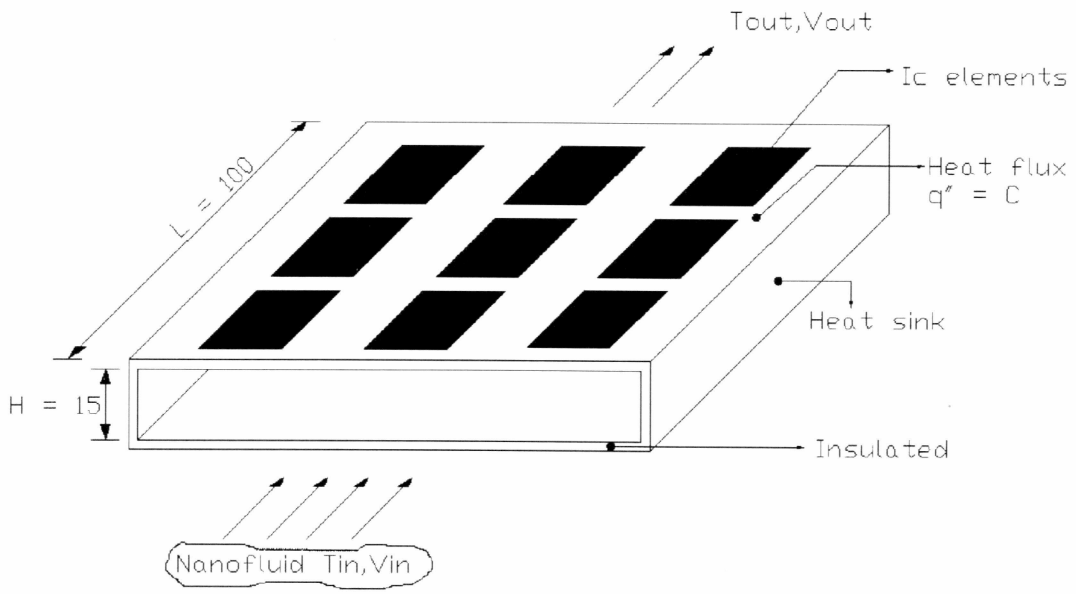

Figure 4.1 Schematic diagram of a cooling arrangement for electronic chips using nanofluids.

Convection of nanofluid consisting of water and CuO nanoparticles in a horizontal rectangular channel with uniform heat flux (q'') at the upper wall has been studied. The domain represents the channels in a heat sink, which is cooling a microprocessor chips placed on the top. Similar arrangements are shown in Incropera and Dewitt [8]. The

problem under investigation is at steady state and the nanofluid flow is maintained in laminar regime.

4.4.1 Assumptions

The nanoparticles in the base fluid may be easily fluidized and consequently the effective mixture behaves like a single phase fluid [2]. It is also assumed that the fluid phase and nanoparticles are in thermal equilibrium with zero relative velocity. This may be realistic as nanoparticles are much smaller than microparticles and the relative velocity decreases as the particle size decreases. The resultant mixture may be considered as a conventional single phase fluid. The properties of the nanofluid are assumed to be constant under the operating conditions and they are evaluated at the fluid inlet temperature T_{in}. From our computations we find T_{in} and T_{out} are fairly close. Therefore using the properties at T_{in} does not introduce too much error. As a refinement properties at the average of T_{in} and T_{out} can be employed. The effective thermophysical properties of the nanofluids are the function of the nanoparticle volume concentration (ϕ) [1]. Furthermore the assumption of single phase for a nanofluid is validated to an extent through the experimental results of Pak and Cho [1] and Xuan and Li [2]. Under these assumptions, the classical theory of single phase fluid can be applied to nanofluid.

4.4.2 Governing equations

For the problem under consideration, nanofluids being liquids are assumed to be incompressible. Also in the energy equation the compression work and viscous dissipation are negligible.

The governing equations for the nanofluid flow under the stated assumptions are;

Continuity:

$$\nabla.(\rho_{nf} V) = 0 \tag{1}$$

Momentum:

$$\nabla.(\rho_{nf} V V_i) = -\nabla p + \nabla.(\mu_{nf} \nabla V_i) \tag{2}$$

Energy:

$$\nabla.(\rho_{nf} V c_{nf} T) = \nabla.(k_{nf} \nabla T) \tag{3}$$

Where ρ_{nf} is density, V is velocity vector, V_i is velocity component, p is pressure, μ_{nf} is viscosity, c_{nf} is specific heat, T is temperature and k_{nf} is thermal conductivity of the nanofluid.

4.4.3 Boundary conditions

The governing equations of the fluid flow are subjected to the following boundary conditions. Fluid enters the channel with uniform axial velocity V_{in}, with a temperature of T_{in}. Outflow boundary condition has been implemented for the outlet. This boundary condition implies zero normal gradients for all flow variables except pressure. On the walls of the channel, the no-slip boundary conditions were imposed. A uniform heat flux (q'') is applied on the upper wall and the lower wall of the channel is assumed to be insulated.

4.5 Thermophysical properties of nanofluids

Thermophysical properties of nanofluids are calculated by using the formulas given by Buongiorno [4].

$$\rho_{nf} = \phi\rho_p + (1-\phi)\rho_{bf} \tag{4}$$

It should be noted that for calculating the specific heat of nanofluid some of prior researchers have used the following correlation

$$c_{nf} = (\phi)c_p + (1-\phi)c_{bf}$$

It is modified in our analysis to the equation (5) presented by Buongiorno which is more accurate.

$$c_{nf} = \frac{\phi\rho_p c_p + (1-\phi)\rho_{bf} c_{bf}}{\rho_{nf}} \tag{5}$$

The thermal conductivity equation (6) was first proposed by Hamilton and Crosser [9] for the mixtures containing micrometer size particles; it is assumed that this equation is applicable for the nanofluids.

$$\frac{k_{nf}}{k_{bf}} = \frac{k_p + (n-1)k_{bf} - (n-1)\phi(k_{bf} - k_p)}{k_p + (n-1)k_{bf} + \phi(k_{bf} - k_p)} \tag{6}$$

Where the subscripts *nf, bf* and *p* refer to nanofluid, base fluid and particles respectively. In the above equation *n* is the shape factor and is equal to 3 for spherical nanoparticles. Viscosity of CuO/water nanofluids with volume concentration $\phi > 5\%$ is calculated from the correlation developed by Kulkarni et al [10]

$$\ln \mu_{nf} = A(\frac{1}{T}) - B \tag{7}$$

Where T is the temperature in Kelvin, A and B are functions of volumetric concentration ϕ. These factors are given by

$$A = 20587\phi^2 + 15857\phi + 1078.3 \text{ with } R^2 = 0.99 \tag{8}$$

$$B = -107.12\,\phi^2 + 53.548\phi + 2.8715 \text{ with } R^2 = 0.97 \quad (9)$$

For nanofluids with ϕ = 2%, viscosity is taken from experiments done on CuO/water nanofluid by Heris et al. [11]. As there is no experimental data on viscosity for CuO/water nanofluids with volume concentration of ϕ = 4%, it was obtained from a curve fit shown in Figure 4.2

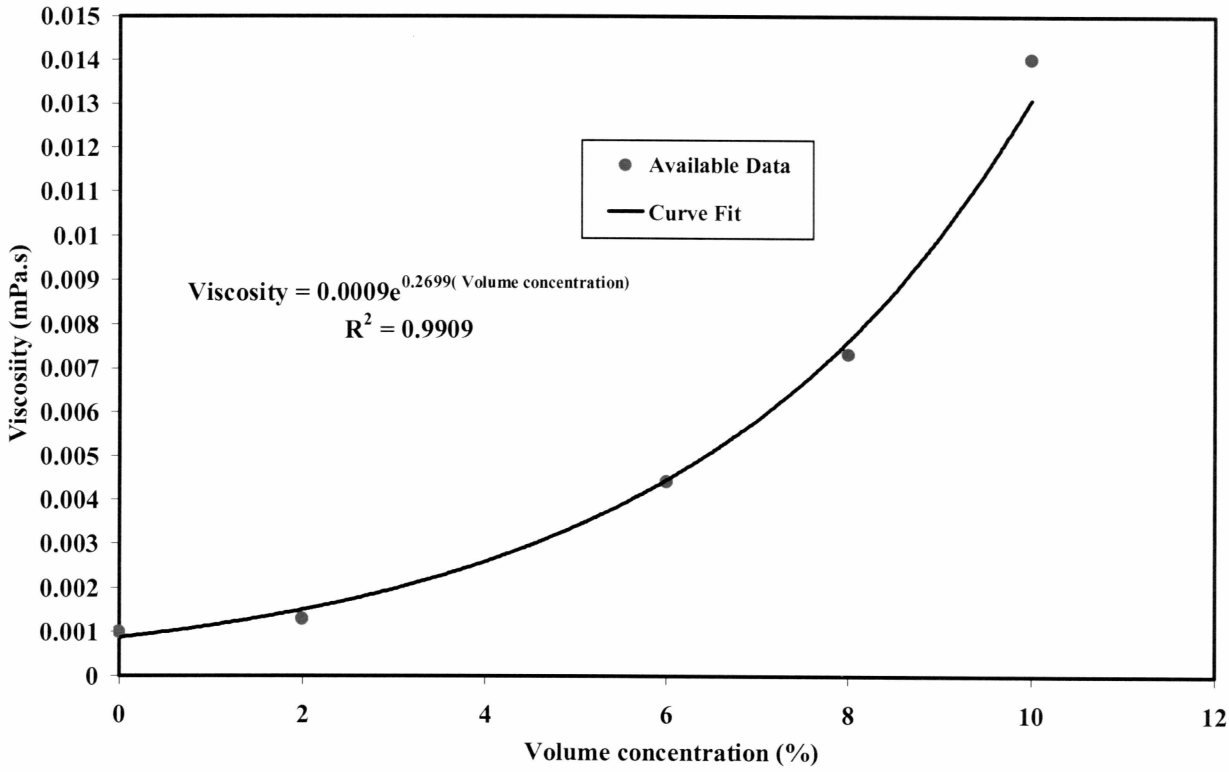

Figure 4.2 Viscosity of CuO nanofluids with varying particle volume concentration.

An exponential curve fit with $R^2 = 0.99$ is used to link the data of Heris et al. [11] (ϕ = 2 %) and the data obtained by Kulkarni et al. [10] (ϕ > 5%). Viscosity for CuO nanofluids with volume concentration 4 % was obtained from the curve fit equation

$$\mu_{nf} = 0.0009e^{(0.2699\phi)}, \text{ For } \quad \phi = 4\% \tag{10}$$

Based on the equations (4) – (10), the properties were calculated and summarized in Table 4.1 These thermophysical properties were used as input in the simulations.

Table 4.1 Thermophysical properties used in the present analysis are evaluated at inlet temperature (Tin) = 293 K.

Particle Volume Percentage (%)	Density (kg/m3)	Thermal Conductivity (W/m2 K)	Viscosity (mPa.s)	Specific Heat (J/kg K)
0	998.20	0.60000	0.0010030	4182.00
2	1156.90	0.63666	0.0013000	3595.63
4	1315.59	0.67465	0.0028000	3150.72
6	1474.29	0.71435	0.0043998	2801.59
8	1632.98	0.75576	0.0073131	2520.33
10	1791.68	0.79901	0.0140087	2288.88

4.6 Numerical method

The computational fluid dynamics code Fluent [12] was used for solving this problem. The system of governing equations (1) – (3) was solved by control volume approach. Control-volume technique converts the governing equations to a set of algebraic equations that can be solved numerically. The control volume approach employs the conservation statement or physical law represented by the entire governing equations over finite control volumes [13]. First order upwind scheme was employed to

discretize for the convection terms, diffusion terms and other quantities resulting from governing equations. Grid schemes used are staggered in which velocity components are evaluated at the center of control volume interfaces and all scalar quantities are evaluated in the center of control volume. Pressure and velocity were coupled using Semi Implicit Method for Pressure Linked Equations [SIMPLE]. Fluent solves the linear systems resulting from discretization schemes using a point implicit (Gauss-Seidel) linear equation solver in conjunction with an algebraic multigrid method. During the iterative process, the residuals were carefully monitored. For all simulations performed in the present study, converged solutions were considered when the residuals resulting from iterative process for all governing equations (1) – (3) were lower than 10^{-8}.

4.7 Model validation

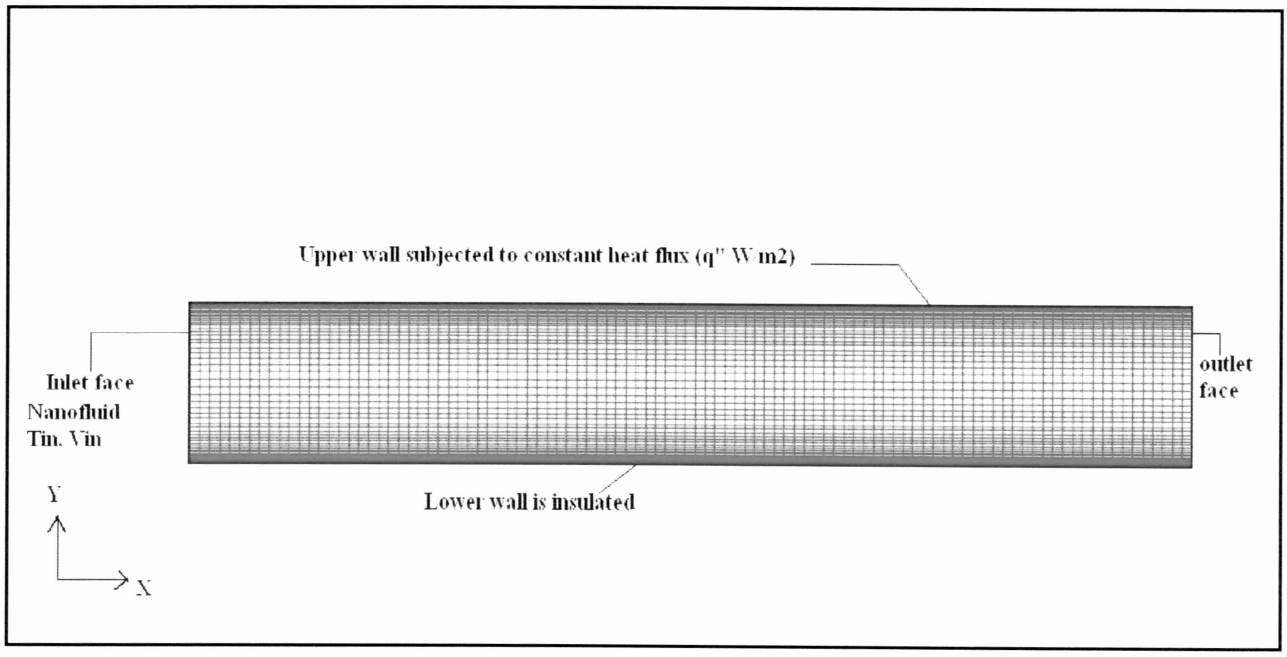

Figure 4.3 Grid layout used in the present numerical study.

4.7.1 Grid sensitivity study

In order to ensure the accuracy as well as the consistency of the numerical results, several grid distributions were tested in the present simulations. The grids were created using the program Gambit [14] which is a preprocessor of Fluent. The selected grid for the present study consisted of 100 in the horizontal (along length) and 50 nodes in the vertical (along height) direction respectively. The axial velocity profile computed at the outlet for Reynolds number 100 is shown in Figure 4.4. The same run was replaced with grid refinement of 150 X 75 nodes and 200 X 100 nodes. Exactly same results are found for refined grids. It is shown in the Figure 4.4 increasing the grid size do not change velocity.

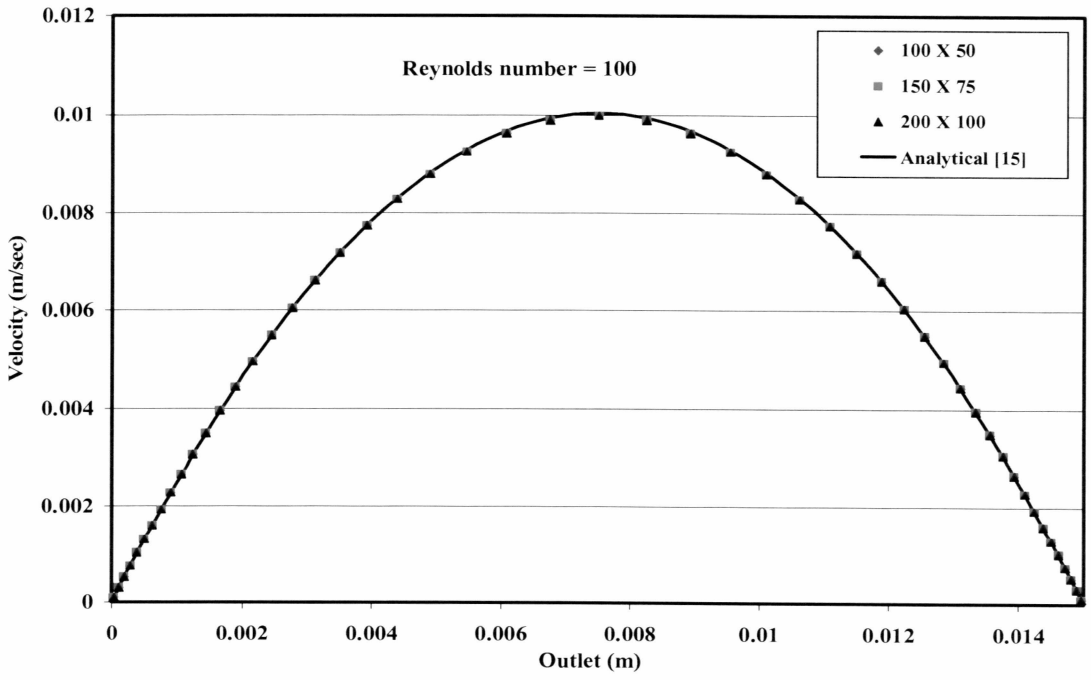

Figure 4.4 Axial velocity profile at outlet for various grid size distributions.

In Figure 4.4 computed velocity profile at the outlet of the parllel plate was compared with the analytical velocity profile for fully developed laminar flow presented in Fox [15]. The computed velocity profile at outlet matched precisely with the analytical profile.

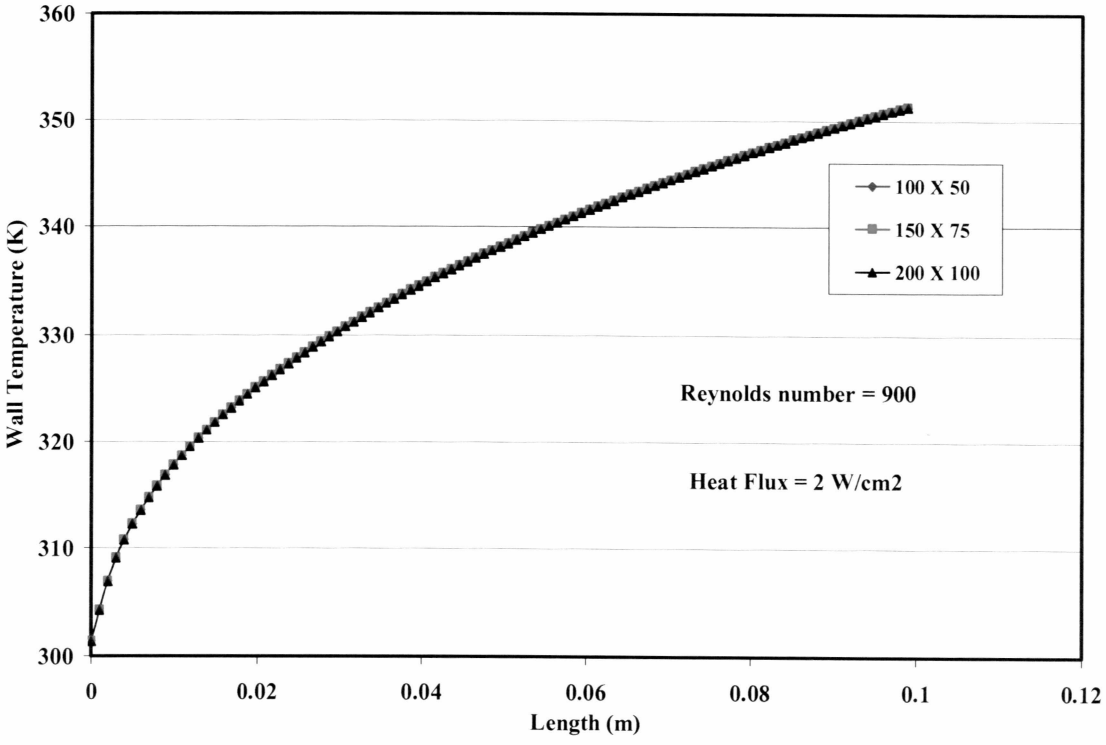

Figures 4.5 Upper wall temperature of the channel along the length for various grid size distributions.

Figure 4.5 shows the grid sensitivity study for temperature calculations. It is conducted at a Reynolds number 900 to limit the upper wall temperature to 85°C since microprocessor

chips are generally maintained in that temperature range. The temperature distribution along the length is seen to be identical for grid distributions 100 X 50, 150 X 75 and 200 X 100. From Figures 4.4 and 4.5 it can be clearly seen that the computed values of the velocity and temperature are not changing significantly as grid size is refined from 100 X 50 to 200 X 100. Therefore the 100 X 50 grid lay out is used in the subsequent computations.

As there exist no experimental data for the present analysis of the nanofluids flow and heat transfer in the parallel plate duct, in order to validate the computational model, the numerical results are compared with the theoretical and numerical data obtained for the conventional fluids. First the local skin friction coefficient in the entrance region is compared with the results presented in Bejan [16].

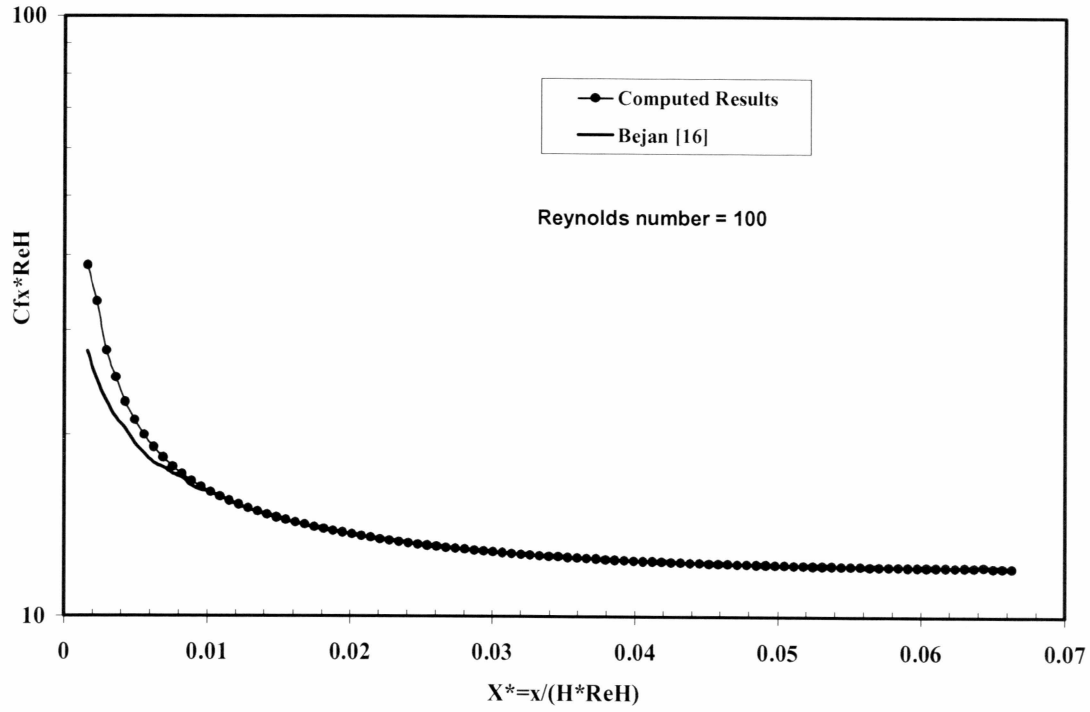

Figure 4.6 Comparison of the local skin friction in the entrance region obtained from numerical analysis with the results presented in Bejan, [$ReH = \frac{\rho VH}{\mu}$].

Figure 4.6 displays the comparison of the local skin friction coefficient (C_{fx}) in the entrance region of the rectangular channel with the results presented in Bejan. The computed values matched closely except at the grid points close to entrance with the theoretical values presented by Bejan. Second the local Nusselt numbers (Nu) in the developing region of flow, while the upper wall is subjected to constant heat flux and the lower wall to zero heat flux obtained from the numerical computation are compared with results presented in Heaton et al. [17].

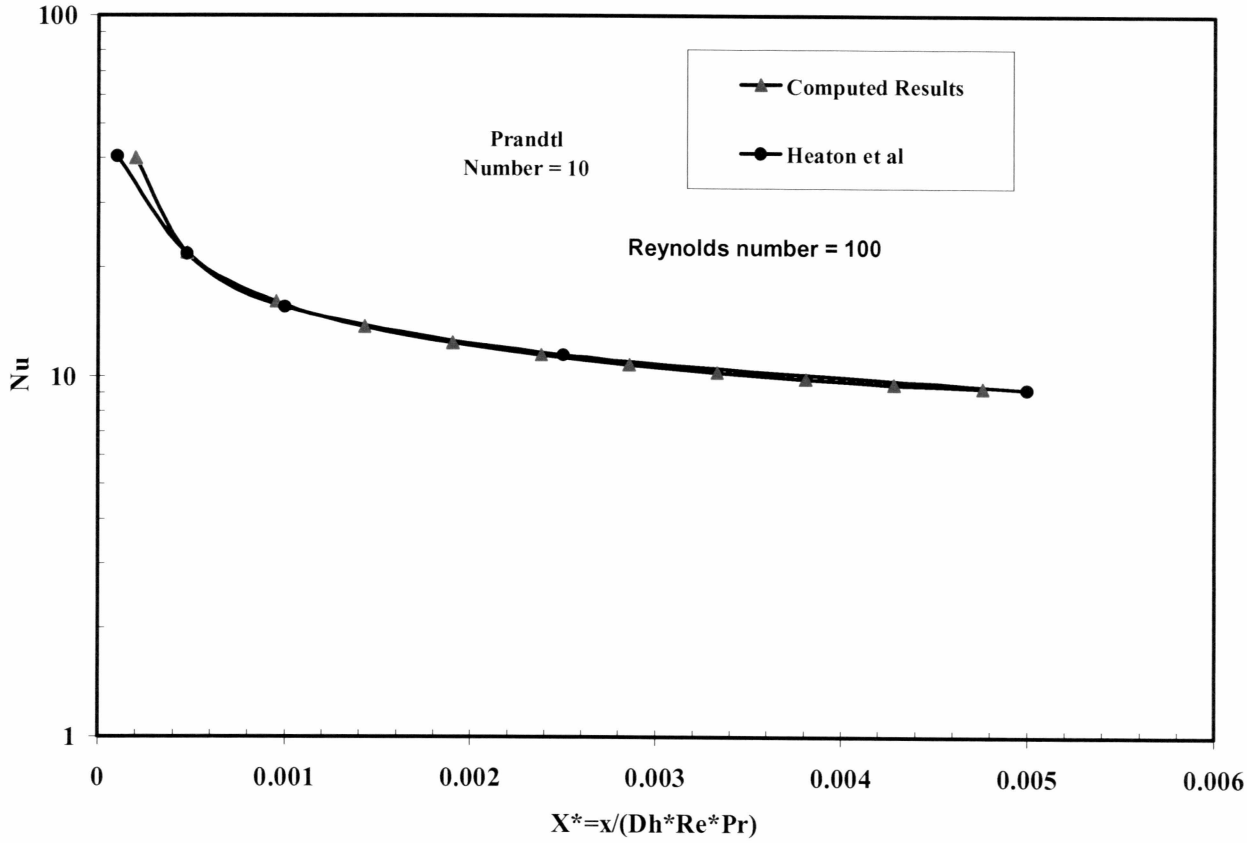

Figure 4.7 Comparison of the local Nusselt number in the entrance region obtained from the numerical computation with the results presented in Heaton et al. [17].

Figure 4.7 displays the comparison of the local Nusselt number in the entrance region obtained from the numerical computation to the results presented by Heaton et al. The numerical results match closely with the theoretical results.

After the above two comparisons and confirming that the computational model is generating correct results, CuO/ water nanofluid with varying concentration from 2% - 10% are analyzed at various Reynolds numbers (*Re*) with applied constant heat flux (q'') on the upper wall and the lower wall being insulated.

4.8 Results

4.8.1 Effect of the nanoparticle concentration on the local Nusselt number

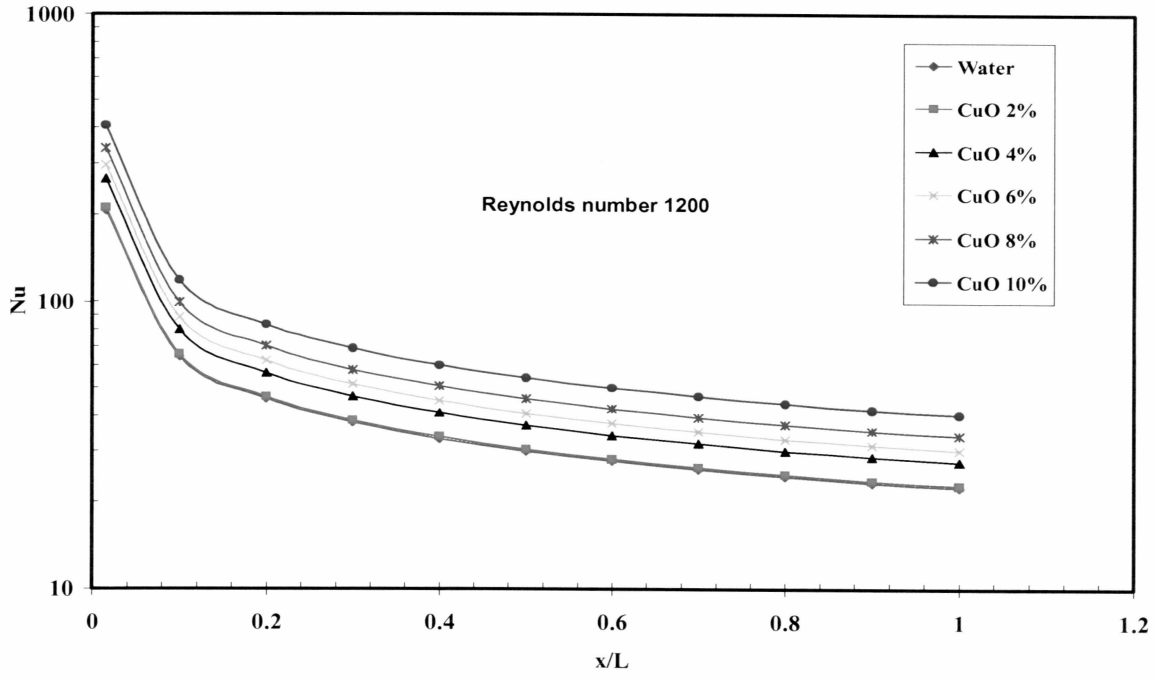

Figure 4.8. The influence of the CuO nanoparticle volume concentration on the local Nusselt number at a fixed Reynolds number of 1200.

From Figure 4.8 it is clearly evident that by adding the nanoparticles to the base fluid the local Nusselt number increases with increase in the particle volume concentration. By adding CuO nanoparticles (10%) to the base fluid water the local Nusselt number increased approximately 2 times at a Reynolds number of 1200. Although the increase in heat transfer coefficient is not apparent between water and 2% CuO nanofluids in Figure 4.8 because of similar Nusselt number, the thermal

conductivity value difference causes the 2% nanofluid to have about 10% higher heat transfer coefficient.

4.8.2 Effect of Reynolds number on the average Nusselt number

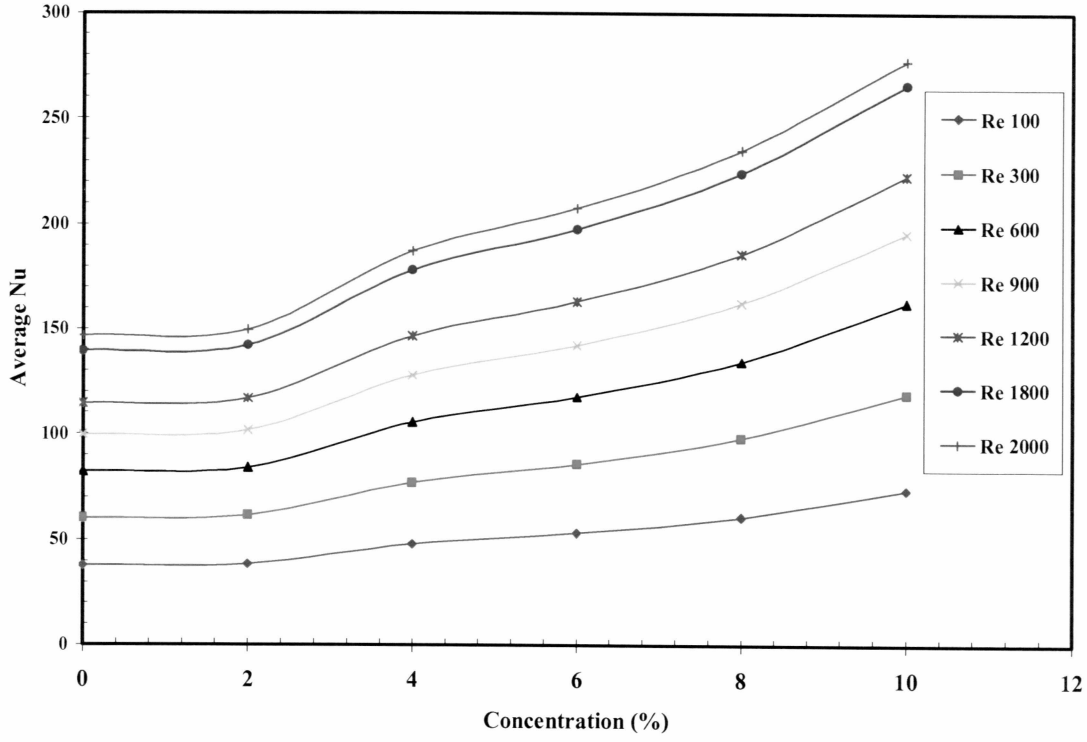

Figure 4.9 Variation of Nu with concentration for an array of Reynolds numbers.

Figure 4.9 shows the average Nusselt number defined as $(\frac{1}{x}\int_0^L Nu)$ increases with the increase in the Reynolds number. The increase is about 3.8 times when the Reynolds number is increased from 100 to 2000. Slight curvature at 4% concentration may be due to lack of precise viscosity data at 4% which we have obtained from the curve-fit Equation 10. We believe that viscosity value used at 4% from Equation (10) is slightly lower than the true value.

4.8.3 Effect of CuO nanoparticle concentration on the local skin friction coefficient

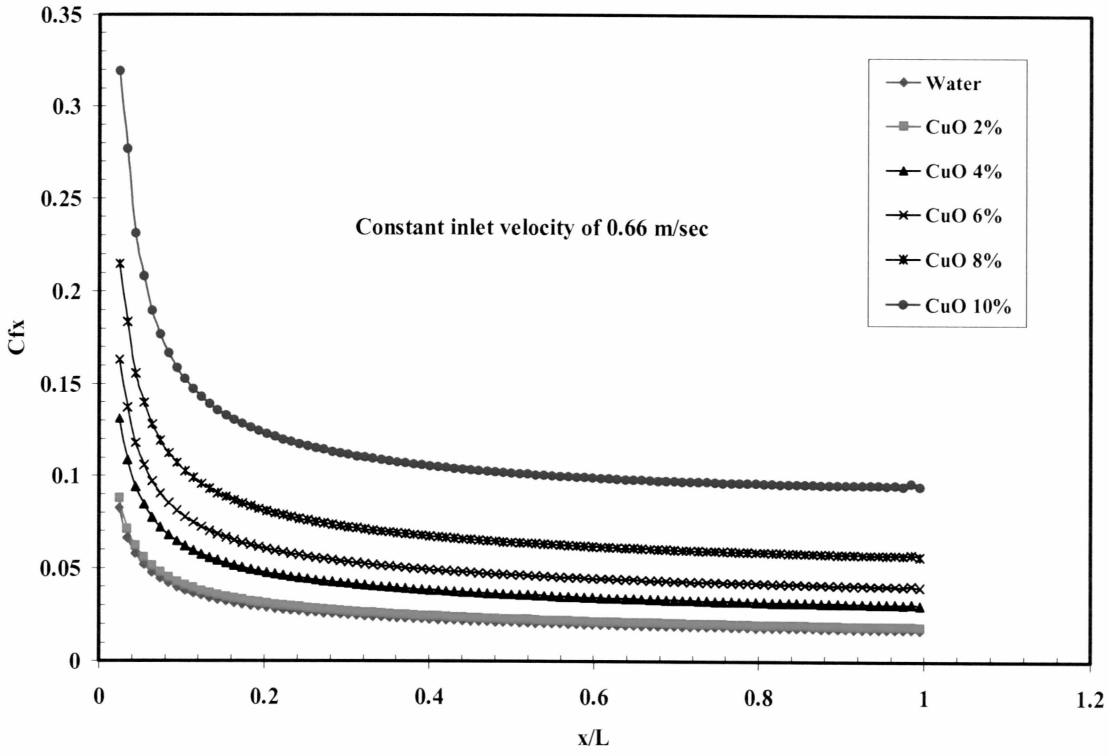

Figure 4.10 The influence of CuO nanoparticle volume concentration on the local skin friction coefficient at a constant velocity of 0.66m/sec.

In Figure 4.10, the variation of local skin friction coefficient is shown along the channel for various CuO nanoparticle concentrations for the same inlet velocity. As the nanoparticle volume concentration increases the skin friction coefficient increases. This results in greater pressure drop across the parallel plate duct. Therefore greater pumping power is required to drive the nanofluids through the duct than the base fluid. This is the major concern for the usage of nanofluids as the next generation heat transfer fluids, and is therefore, explored below.

4.9 Evaluation of the pumping power of CuO nanofluids

At a fixed Reynolds number, the heat transfer coefficient increases and also the pressure drop. A careful analysis should be carried out when choosing a nanofluid of certain concentration as a heat transfer agent for a particular application.

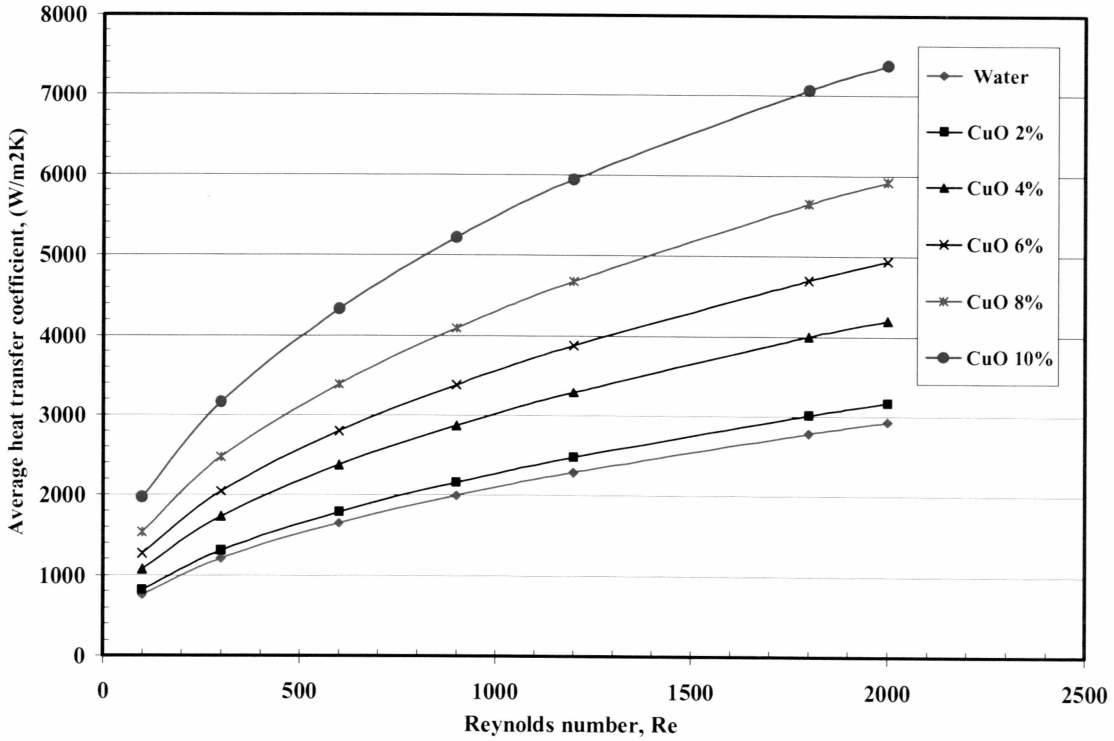

Figure 4.11 The influence of CuO nanoparticle volume concentration and the Reynolds number on the average heat transfer coefficient.

Figure 4.11 was generated by running the computational model at Reynolds numbers 100 to 2000 to span the complete laminar range. The average heat transfer coefficients ($\frac{1}{x}\int_0^L h$) are obtained from computations and were plotted. At a Reynolds number of 2000, the

base fluid water has an average heat transfer coefficient of 2930 W/m^{2}K. Taking this as a reference, an analysis is carried out for a constant heat transfer coefficient of this magnitude for the CuO nanofluids with various concentrations from 2% to 10%. From Figure 4.11 the corresponding Reynolds numbers for this same heat transfer coefficient of 2930 W/m^{2}K of different concentration of CuO nanofluids were found. From the calculated Reynolds numbers, velocities were determined. Corresponding average skin friction coefficient ($C_f = \frac{1}{x}\int_0^L C_{fx}$) was obtained from computations at various Reynolds numbers from 100 to 2000. Then the corresponding pumping power was calculated.

The results are summarized in Table 4.2. It can be observed that for same heat transfer coefficient 2930 W/m^{2}K, water has the highest Reynolds number of 2000 and CuO nanofluid with 10% volume concentration has the least Reynolds number of 259. Corresponding velocities and the volume flow rates are calculated.

$$\dot{V} = AV \tag{11}$$

Average skin friction coefficient (C_f) is computed from the existing computational model. Then the pressure drop in the channel is calculated using

$$\Delta P = \frac{\rho L V^2 4C_f}{D_h} \tag{12}$$

The power required to pump the fluid is then calculated using

$$\text{Power} = \Delta P \dot{V} \tag{13}$$

To confirm the developing flow conditions, the hydrodynamic and thermal entry lengths for the parallel plate duct with various concentrations of nanofluids were calculated by using formulas from Incropera and Dewitt [8].

$$\text{Hydrodynamic entry length} = 0.011 Re D_h \tag{14}$$

$$\text{Thermal entry length} = 0.012 Re Pr D_h \tag{15}$$

The hydrodynamic and thermal entry lengths are decreasing with increase in concentration of nanofluids to maintain the same level of heat transfer. The Prandtl number increase is moderate where as the Reynolds number decrease is much stronger.

It is observed from Table 4.2 that for the same heat transfer coefficient 2930 W/m^2K considered, nanofluids require higher power than the base fluid. This is because the nanofluids have higher viscosity. This analysis clearly shows that using higher concentrations (greater than 2%) of nanofluid under laminar flow condition can demand high pumping power

Table 4.2 Comparison of the performance of various CuO nanofluids with base fluid water.

Concentration (%)	0	2	4	6	8	10
Heat Transfer Coefficient (W/m2 K)	2930	2930	2930	2930	2930	2930
Reynolds Number	2000	1700	935	665	442	259
Hydrodynamic Entrance Length (m)	0.66	0.561	0.30855	0.21945	0.14586	0.08547
Prandtl Number	6.99	7.34	13.08	17.26	24.39	40.13
Thermal Entrance Length (m)	5.0335	4.4933	4.4015	4.1310	3.8806	3.7417
Velocity (m/s)	0.0670	0.0637	0.0663	0.0662	0.0660	0.0675
Average Skin fiction Coefficient	0.03731	0.04156	0.06252	0.07958	0.10725	0.16148
Pressure Loss (Pa)	1.114	1.300	2.413	3.423	5.083	8.789
Volumetric Flow Rate (m3/s)	0.00100	0.00096	0.00099	0.00099	0.00099	0.00101
Power (W)	0.0011	0.0012	0.0024	0.0034	0.0050	0.0089
Power Ratio	1.0	1.1	2.1	3.0	4.5	7.9

Table 4.2 summarizes important findings from these simulations for flows in the hydrodynamically and thermally developing fields in laminar flow. Comparisons between base fluid and CuO nanofluids of various concentrations with regards to heat transfer and pressure loss have been investigated and summarized in Table 4.2. Similar studies should be beneficial for nanofluid selection.

4.10 Conclusions

The following conclusions are drawn from this study.

1. A grid sensitivity analysis yields that a 100 X 50 grid size (100 grid points in X- direction and 50 in Y- direction) is adequate to exactly reproduce the velocity profile at the outlet and the upper wall temperature distribution.
2. Comparisons between computed results for skin friction and Nusselt number agree well with the theoretical results of Bejan [16] and Heaton et al [17] respectively.
3. Nusselt number computations for CuO nanofluids with varying particle volume concentrations exhibit substantial increase of Nusselt number with concentration. For example at a constant Reynolds number of 1200 the Nusselt number increases by 2 times for CuO nanofluid of 10% volume concentration.
4. Nusselt number is function of Reynolds number and Prandtl number. At a constant Reynolds number, Nusselt number increases with concentration. Because from the thermophysical properties calculation we observed that the Prandtl number increases with concentration. The increase in Prandtl number causes the increase in Nusselt number.
5. The average Nusselt number for flow in a parallel plate duct as a function of Reynolds number and concentration has been numerically analyzed. This analysis for nanofluids show that Nusselt number increases with Reynolds

number and also with particle volume concentration. However, the influence of Reynolds number is stronger. For example, Nusselt number increases from 73 to 277 for Reynolds number 100 to 2000 for a particle concentration of 10%. This increase is less at a lower particle concentration.

6. For constant inlet velocity an increase in particle volume concentration results in much higher skin friction coefficient along the duct. The average skin friction coefficient of 10% CuO nanofluid in the fully developed region is about 4 times compared to the pure water at a constant inlet velocity of 0.66 m/sec.
7. The average heat transfer coefficient in the modeled duct with pure water is 2930 W/m^2K at a Reynolds number 2000 whereas for CuO nanofluid with 10% concentration, it is 7378 W/m^2K. However, this increase in heat transfer coefficient due to concentration change is smaller at lower Reynolds number. Prandtl number increases with concentration which causes the increase in Nusselt number.
8. For a fixed value of heat transfer coefficient for the computed parallel plate geometry a Reynolds number of 259 for CuO nanofluid (10%) achieves the same heat transfer coefficient at Reynolds number 2000 for pure water. It is noteworthy from the tabular results that due to the change in viscosity and density of nanofluids, which are highly dependent on the concentration, the velocity in the passage is nearly constant despite the change in Reynolds number from 259 to 2000. The average skin friction and the pressure loss

steadily increase with concentration. The pumping power increases substantially. Therefore in order to receive the benefit of nanofluids for heat transfer under laminar flow regime, the nanofluids may be limited to lower concentrations or if the nanofluid can be heated up substantially lowering the viscosity then the pressure loss can be reduced.

4.11 Nomenclature

x	Distance from the inlet, m
L	Length, m
H	Height, m
A	Area, m^2
D_h	Hydraulic diameter, $2H$
T	Temperature, K
q''	Heat flux, W/m^2
V	Velocity, m/sec
c	Specific heat, J/kg.K
k	Thermal conductivity, W/m.K
C_{fx}	Local skin friction coefficient
Nu	Nusselt number
Re	Reynolds number
$\dot{V}$	Volume flow rate, m^3/sec
ΔP	Pressure drop, N/m^2

Greek Letters

ϕ	Volume concentration
ρ	Density, kg/m^3
μ	Viscosity, mPa.s

Subscripts

p	Nanoparticle
nf	Nanofluid
bf	Base fluid
in	Inlet
out	Outlet

4.12 Acknowledgements

Financial assistance from the Arctic Region Supercomputing Center (ARSC) and the Department of Mechanical Engineering at the University of Alaska Fairbanks is gratefully acknowledged.

4.13 References

[1] B. C. Pak, Y. I. Cho, Hydrodynamic and heat transfer study of dispersed fluids with submicron metallic oxide particles, Experimental Heat Transfer 11 (1998) 151-170.

[2] Y. Xuan, Q. Li, Investigation on convective heat transfer and flow features of nanofluids, ASME Journal of Heat Transfer 125 (2003) 151-155.

[3] Y. Yang, Z. G. Zhang, E. A. Grulke, W. B. Anderson, G. Wu, Heat transfer properties of nanoparticle-in-fluid dispersions (nanofluids) in laminar flow, International Journal of Heat and Mass Transfer 48 (2005) 1107-1116.

[4] J. Buongiorno, Convective transport in nanofluids, ASME Journal of Heat Transfer 128 (2006) 240-250.

[5] A. Akbarinia, A. Behzadmer, Numerical study of laminar mixed convection of a nanofluid in horizontal curved tubes, Applied Thermal Engineering 27 (2007) 1327-1337.

[6] S. B. Maiga, S. J. Palm, C. T. Nguyan, G. Roy, N. Galanis, Heat transfer enhancement by using nanofluids in forced convection flows, International Journal of Heat and Fluid Flow 26 (2005) 530-546.

[7] A. Behzadmer, M. S. Avval, N. Galanis, Prediction of turbulent forced convection of a nanofluid in a tube with uniform heat flux using two phase approach, International Journal of Heat and Fluid Flow 28 (2007) 211-219.

[8] F. P. Incropera, D. P. Dewitt, Introduction to heat transfer, John Wiley and Sons, New York, 2001.

[9] R. L. Hamilton, O. K Crosser, Thermal conductivity of heterogeneous two-component system, I and EC Fundamentals 1 (1962) 187-191.

[10] D. P. Kulkarni, D. K. Das, G. A. Chukwu, Temperature dependent rheological property of copper oxide nanoparticles suspension, Journal of Nanoscience and Nanotechnology 6 (2006) 1150-1154.

[11] S. Z. Heris, M. N. Esfahany, G. Etemad, Investigation of CuO/Water nanofluid laminar convective heat transfer through a circular tube, Journal of Enhanced Heat Transfer 13 (2006) 279-289.

[12] Fluent 6.2 user guide, Fluent Inc, Lebanon, New Hampshire, 2005.

[13] S. V. Patankar, Numerical heat transfer and fluid flow, Hemisphere Publishing Corporation, New York, 1980.

[14] Gambit user guide, Fluent Inc, Lebanon, New Hampshire, 2005.

[15] R. W. Fox, A. T. McDonald, Introduction to Fluid Mechanics, John Wiley & Sons, New York, 1992.

[16] A. Bejan, A. D. Kraus, Heat transfer handbook, John Wiley & Sons, New Jersey, 2003.

[17] H. S. Heaton, W. C. Reynolds, W. M. Kays, Heat transfer in annular passages simultaneous development of velocity and temperature fields in laminar flow, International Journal of Heat and Mass Transfer 7(1964) 763-781.

Chapter Five

Numerical Study of Turbulent Flow and Heat Transfer Characteristics of Nanofluids Considering Variable Properties

5.1 Abstract

Turbulent flow and heat transfer of three different nanofluids (CuO, Al_2O_3 and SiO_2) in an ethylene glycol and water mixture flowing through a circular tube under constant heat flux condition have been numerically analyzed. New correlations for viscosity upto 10% volume concentration for these nanofluids as a function of volume concentration and temperature are developed from the experiments and are summarized in the present paper. In our numerical study, all the thermophysical properties of nanofluids are temperature dependent. Computed results are validated with existing well established correlations. Nusselt number prediction for nanofluids agrees well with Gnielinski correlation. It is found that nanofluids containing smaller diameter nanoparticles have higher viscosity and Nusselt number. Comparison of convective heat transfer coefficient of CuO, Al_2O_3 and SiO_2 nanofluids have been presented. At a constant Reynolds number, Nusselt number increases by 35% for 6% CuO nanofluids over the base fluid.

---

*Namburu. P.K. and Das. D.K. 2007. Numerical Study of Turbulent Flow and Heat Transfer Characteristics of Nanofluids Considering Variable Properties. In Review. International Journal of Heat and Fluid Flow.

5.2 Keywords

Nanofluid; Nanoparticles; Viscosity; Turbulent flow; Heat transfer enhancement; Convection

5.3 Introduction

Nanofluids are created by dispersing nanometer-sized particles (<100 nm) in a base fluid such as water, ethylene glycol or propylene glycol. Using high thermal conductivity metallic nanoparticles (e.g., copper, aluminum, silver and silicon) increases the thermal conductivity of such mixtures, thus enhancing their overall energy transport capability (Xuan and Li, 2003). Nanofluids have attracted attention as a new generation of heat transfer fluids in building heating, in heat exchangers, in plants and in automotive cooling applications, because of their excellent thermal performance. Various benefits of the application of nanofluids include: improved heat transfer, heat transfer system size reduction, minimal clogging, microchannel cooling & miniaturization of systems (Choi, 1995). Therefore, research is underway to apply nanofluids in environments where higher heat flux is encountered and the conventional fluid is not capable of achieving the desired heat transfer rate.

A great deal of energy is expended heating residential and industrial buildings in the cold regions of the world. Due to the severe winter conditions, ethylene glycol or propylene glycol mixed with water in different volume percentages are typically used to lower the aqueous freezing point of the heat transfer medium (McQuiston et al., 2000). Such heat transfer fluids are used in heat exchangers, baseboard heaters in homes, automobiles and in industrial plants in cold regions. These fluids can withstand low

temperatures down to - 60°C. At low temperatures, ethylene glycol mixtures have better heat transfer characteristics than propylene glycol mixtures (ASHRAE, 2005). A 60% ethylene glycol and 40% water by weight fluid mixture is most commonly used in the sub-arctic and arctic regions of Alaska.

In order to evaluate the superior heat transfer characteristics of nanofluids there must be ample data on the thermophysical properties of such fluids. Eastman et al. (2001) observed that with 0.3% volume concentration of copper nanoparticles dispersed in ethylene glycol, its thermal conductivity increased by 40%. Das et al. (2003) have reported a 10 – 25% increase in thermal conductivity with 1- 4% volume concentration of alumina nanoparticles in water. Kulkarni et al. (2007) reported that the experimental viscosity values of Copper oxide (CuO) dispersed in propylene glycol and water mixture are much higher than those predicted by Batchelor (1977) equation. A review article by Wang and Mujumdar (2007) lists studies conducted on the thermal conductivity and heat transfer of various nanofluids. However, no universal correlations have been developed thus far to calculate the properties of all types of nanofluids of all concentrations.

Pak and Cho (1998) performed viscosity, pressure loss and heat transfer measurements on titanium dioxide nanofluids up to 3% concentration by volume and found single-phase correlations can be successfully extended to nanofluids. They reported increase in the convective heat transfer coefficient with particle volume concentration and Reynolds number. They also reported Nusselt numbers increased by 30% over the Dittus – Boelter (1930) equation for single phase fluids. A new single phase

correlation for the turbulent convective heat transfer for dilute concentration of nanofluids was proposed by them.

$$Nu = 0.021\, Re^{0.8}\, Pr^{0.5} \qquad (1)$$

For $6.54 \leq Pr \leq 12.33$; $10^4 \leq Re \leq 10^5$

Xuan and Li (2003) performed experimental study on Cu-water nanofluids up to 2% volume concentration and developed a Nusselt number correlation. They found that Cu-water dilute nanofluids have almost same pressure drop as water under the same Reynolds number. Heris et al. (2006) performed laminar convective heat transfer experiments on CuO/water and aluminum oxide (Al_2O_3)/water nanofluids and concluded that the heat transfer enhancement by nanofluids depends on several factors including increment of thermal conductivity, nanoparticle type, size, base fluid, flow regime and the boundary conditions. Nguyen et al. (2007) experimentally investigated the heat transfer characteristics of Al_2O_3/water nanofluids for an electronic cooling application. They found the heat transfer coefficient with 6.8% particle volume concentration increased as much as 40% compared to the base fluid.

Maiga et al. (2005) conducted a numerical study on γ - Al_2O_3 nanofluids flow under forced laminar convection in circular tubes and between parallel disks. For a range of Reynolds number from 250 to 1000 they concluded that the heat transfer enhancement is much more pronounced with the increase in particle concentration. However, they observed a drastic adverse effect on wall shear stress in comparison to the base fluid. For the analysis of flow between discs, they found insignificant effect on heat transfer with the variation of gap between the discs. Akbarinia and Behzadmehr (2007) presented a

numerical study of nanofluids under mixed laminar convection in a curved tube. They compared the variations of Nusselt number with Grashof number for various volume percentages of Al_2O_3 nanoparticles in water. They found that at large Grashof number the skin friction was reduced. A second study by Maiga et al. (2006) presented the numerical study of hydrodynamic and thermal behaviors of fully developed turbulent flow of nanofluids Al_2O_3/water nanofluids inside a circular tube subjected to a uniform heat flux of 50 W/cm^2. A new correlation for Nusselt number was derived from their study.

$$Nu = 0.085\, Re^{0.71}\, Pr^{0.35} \qquad (2)$$

For $6.6 \leq Pr \leq 13.9;\ 10^4 \leq Re \leq 5\ X\ 10^5$

EG/water based nanofluids are required for application in cold regions, which have not been studied widely thus far. Since the sub zero temperature operation needed the rheological properties, viscosity measurements of various nanofluids have been investigated. New viscosity correlations as a function of temperature and volume concentration for SiO_2 and Al_2O_3 nanoparticles in EG/ water base fluid was presented. The present paper covers the rheological investigations of nanofluids up to 10% volume concentration and heat transfer computation up to 6%. Using the rheological properties we have presented numerical computations for turbulent forced convection, which will be useful in the design of heat transfer systems in cold climates. Comparisons of the computed Nusselt number with the correlations developed by Pak and Cho (1998) and Maiga et al. (2006) have been presented. Furthermore, the previous investigations limited to dilute concentration up to 3%. In the present study the Prandtl number are in much higher range 47 $\leq$Pr $\leq$105 than those reported by the earlier researchers.

5.4 Thermophysical properties of nanofluids

Thermophysical properties of nanofluids are calculated by using the formulas summarized by Buongiorno (2006).

$$\rho_{nf} = \phi\rho_p + (1-\phi)\rho_{bf} \tag{3}$$

It should be noted that for calculating the specific heat of nanofluid some of prior researchers have used the following correlation

$$c_{nf} = \phi c_p + (1-\phi)c_{bf} \tag{4}$$

It is modified in our analysis to the equation (5) presented by Buongiorno (2006) which is more accurate.

$$c_{nf} = \frac{\phi\rho_p c_p + (1-\phi)\rho_{bf} c_{bf}}{\rho_{nf}} \tag{5}$$

The most commonly used thermal conductivity equation (6) was proposed by Hamilton and Crosser (1962) for the mixtures containing micrometer size particles; it is assumed that this equation is applicable for the nanofluids.

$$\frac{k_{nf}}{k_{bf}} = \frac{k_p + (n-1)k_{bf} - (n-1)\phi(k_{bf} - k_p)}{k_p + (n-1)k_{bf} + \phi(k_{bf} - k_p)} \tag{6}$$

In the above equation n is the shape factor and is equal to 3 for spherical nanoparticles.

The properties of base fluid, EG/Water at different temperatures ($\geq$293 K) are available in ASHRAE (2005). These properties as a function of temperature were curve fitted from ASHRAE data. Then they were substituted in the density, specific heat, thermal conductivity equations (3), (5) and (6) to evaluate the properties of nanofluid at different temperatures and concentrations. Therefore, in our simulations the properties of

nanofluids are temperature dependent. The properties of solid particles are taken to be constant in the present operating range of 293 K to about 363 K, the highest encountered temperature near the wall that occurs at a Reynolds number of 10^4.

Viscosity of CuO/EG water nanofluids with particle diameter of (29 nm) with volume concentration 1 - 6% is calculated from the correlation developed by Namburu et al. (2007).

$$\text{Log } \mu_{nf} = Ae^{-BT} \tag{7}$$

where T is the temperature in Kelvin, and ranging from 238 K (-35°C) to 323 K (50°C) and A and B are functions of volumetric concentration ϕ. The factors A and B are given by

$$A = 1.8375(\phi)^2 - 29.643(\phi) + 165.56 \text{ with } R^2 = 0.9873 \tag{8}$$

$$B = 4 \times 10^{-6}(\phi)^2 - 0.001(\phi) + 0.0186 \text{ with } R^2 = 0.9881 \tag{9}$$

In the above expressions ϕ ranges from 0 to 6.12.

Viscosity values of silicon dioxide (SiO_2) /EG water nanofluids (20 nm, 50 nm and 100 nm) were measured for 2 – 10% volume concentrations on a Brookfield LV DV-II+ viscometer (1999). From the experimental viscosity values, a correlation for 50 nm SiO_2 nanofluids was developed similar to Equation (7) that related nanofluid viscosity with particle volume concentration and the temperature of the nanofluid.

where T is the temperature in Kelvin in the same range as Equation (7) and A and B are functions of volumetric concentration ϕ. These factors are given by

$$A = 0.1193(\phi)^3 - 1.9289(\phi)^2 - 2.245(\phi) + 167.17 \text{ with } R^2 = 0.981 \tag{10}$$

$$B = -7 \times 10^{-6} (\phi)^2 - 0.0004 (\phi) + 0.0192 \text{ with } R^2 = 0.99 \quad (11)$$

In the above expression, ϕ ranges from 2 to 10.

5.4.1 Particle diameter effect on the viscosity of nanofluids

From our experiments on the viscosity of SiO_2 nanofluids of different particle diameters 20 nm, 50 nm and 100 nm exhibited in Figure 5.1, we observed that the nanoparticles of smaller diameter posses the higher viscosity for the same volume concentration of nanofluids. This is physically quite realistic because for a given volume concentration, smaller diameter nanoparticles will be more in number and the total surface area of these smaller diameter nanoparticles will be more. Therefore, smaller diameter nanoparticles interact with the surrounding fluid over a greater surface area, thus increasing the viscosity.

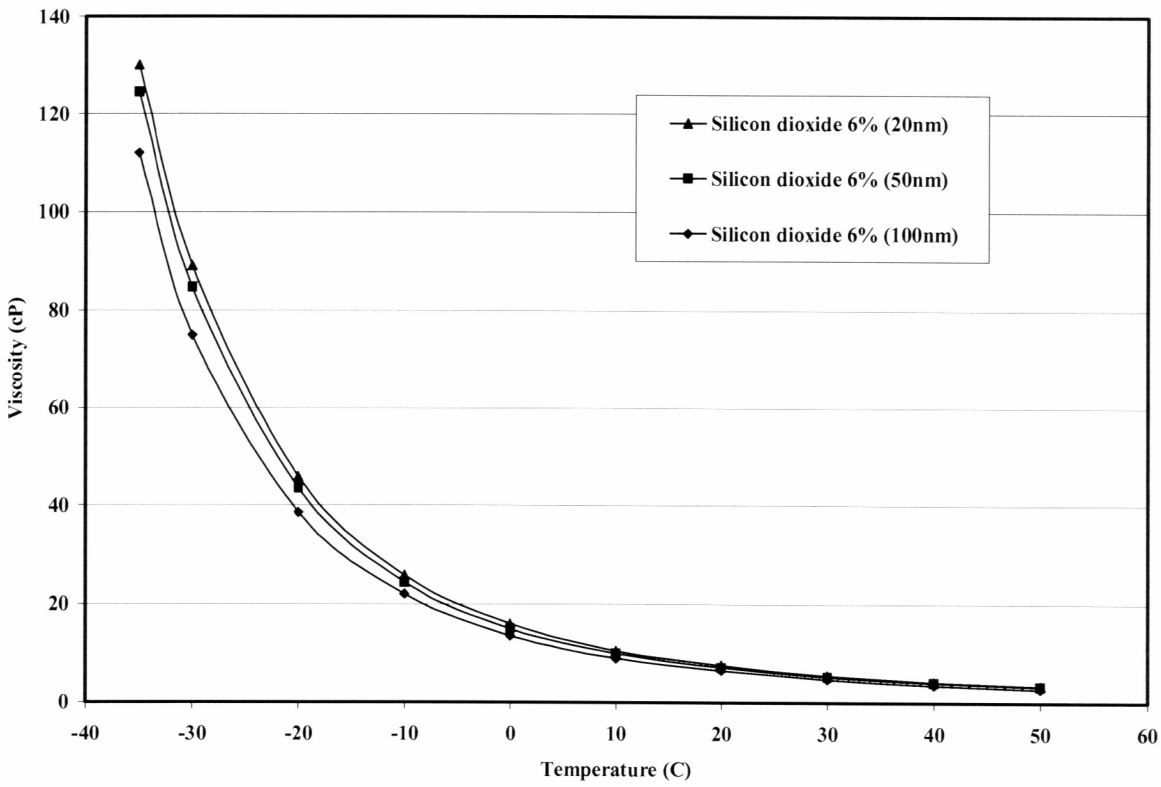

Figure 5.1 Effect of nanoparticle diameter on the viscosity of SiO2 nanofluids with 6% volume concentration.

This is an interesting result regarding the influence of nanoparticle size on viscosity of nanofluids and believed to be reported for the first time.

Viscosity values of aluminum oxide (Al_2O_3)/EG water nanofluids (53 nm) were measured for 1 – 10% volume concentrations. From the experimental data a correlation was developed that related nanofluid viscosity with particle volume concentration and the temperature of the nanofluid, similar to Equation (7).

where T is the temperature in Kelvin in the same range as in Equation (7) and A and B are functions of volumetric concentration ϕ. These factors are given by

$$A = -0.29956(\phi)^3 + 6.7388(\phi)^2 - 55.444(\phi) + 236.11 \text{ with } R^2 = 0.9978 \quad (12)$$

$$B = (-6.4745(\phi)^3 + 140.03(\phi)^2 - 1478.5(\phi) + 20341)/10^6 \text{ with } R^2 = 0.9994 \quad (13)$$

In the above expression, ϕ ranges from 1 to 10.

An effort to combine the viscosity correlations of three nanofluids to a single equation was not successful. All the thermophysical properties discussed above were incorporated in the present numerical analysis to compute the turbulent heat transfer for three different types of nanofluids. As an example, the inclusion of properties variations in our computational analysis is illustrated in Table 5.1 for one temperature.

Table 5.1 Thermophysical properties of the nanofluids used in the numerical computations at inlet temperature of 293 K.

Type of fluid	Volume concentration (%)	Viscosity (mPa.s)	Density (kg/m3)	Specific heat (J/kg.K)	Thermal conductivity (W/m.K)	Prandtl number
EG/water (Base Fluid)	0	5.38	1086.27	3084.00	0.349	47.54
CuO/EG water	1	6.15	1138.51	2942.61	0.359	50.40
CuO/EG water	2	6.83	1190.74	2813.63	0.369	52.04

CuO/EG water	3	9.08	1242.98	2695.50	0.380	64.46
CuO/EG water	4	11.38	1295.22	2586.89	0.390	75.42
CuO/EG water	5	14.00	1347.46	2486.70	0.401	86.78
CuO/EG water	6	18.75	1399.69	2393.99	0.424	105.82
SiO_2/EG water (20 nm)	6	7.58	1154.29	2814.09	0.381	55.97
SiO_2/EG water (50 nm)	6	7.16	1154.29	2814.09	0.381	52.87
SiO_2/EG water (100 nm)	6	6.53	1154.29	2814.09	0.381	48.22
Al_2O_3/EG water	6	9.67	1259.29	2645.35	0.425	60.23

Notice the dominate change of viscosity with concentration. The Prandtl number which greatly influences heat transfer is also varying over a large range for the three nanofluids shown.

5.5 Mathematical modeling

5.5.1 Assumptions

The nanoparticles in the base fluid may be easily fluidized and consequently the effective mixture behaves like a single phase fluid (Xuan and Li, 2003). It is also assumed that the fluid phase and nanoparticles are in thermal equilibrium with zero relative velocity. This may be realistic as nanoparticles are much smaller than microparticles and the relative velocity decreases as the particle size decreases. The resultant mixture may be considered as a conventional single phase fluid. The thermal and physical properties are temperature dependent under the operating conditions. The effective thermophysical properties are dependent upon the temperature and volume concentration. Furthermore the assumption of single phase for a nanofluid is validated to an extent through the experimental results of Pak and Cho (1998) and Xuan and Li (2003). Under these assumptions, the classical theory of single phase fluid can be applied to nanofluids.

5.5.2 Governing equations

The problem under investigation is steady, forced turbulent convection flow of nanofluid flowing inside a straight circular tube having diameter of 0.01 m and a length of 0.8 m. The fluid enters the circular tube with uniform axial velocity and temperature. The flow and thermal fields are assumed to be symmetrical with respect to the horizontal plane parallel to x- axis as shown in Figure 5.2.

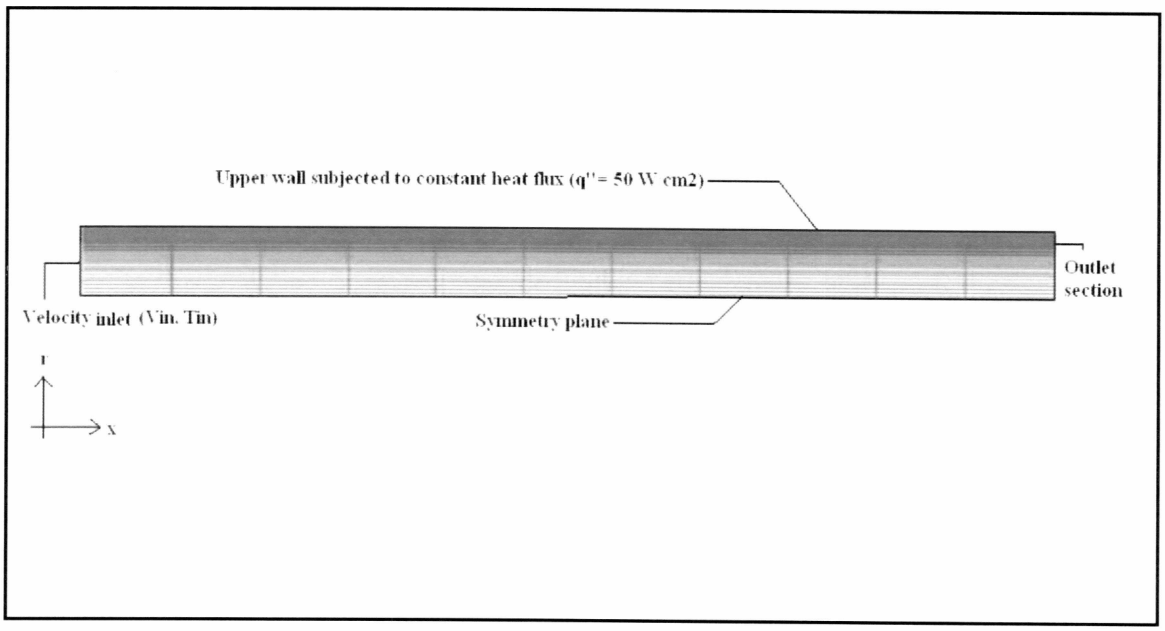

Figure 5.2 Grid layout used in the present analysis.

The governing equations for the fluid flow are (Shih, 1984);

$$div(\rho\overline{V}) = 0 \tag{14}$$

$$div(\rho\overline{V}\overline{V}) = -grad(\overline{P}) + \mu\nabla^2\overline{V} - div(\rho\overline{u}\overline{u}) \tag{15}$$

$$div(\rho\overline{V}c_p\overline{T}) = div(kgrad\overline{T} - \rho c_p\overline{u}\overline{t}) \tag{16}$$

In the above equations, the symbols $\overline{V}$, $\overline{P}$ and $\overline{T}$ represent the time averaged flow variables, while the symbols $\bar{u}$ and $\bar{t}$ represent the fluctuations in velocity and temperature. The terms in the governing equations $\rho\overline{\bar{u}\bar{u}}$ and $\rho c_p\overline{\bar{u}\bar{t}}$ represent the turbulent shear stress and turbulent heat flux. These terms are unknown and must be approximately expressed in terms of mean velocity and temperature.

5.5.3 Turbulence modeling

For closure of the governing equations of fluid flow, empirical data or approximate models are required to express the turbulent stresses and heat flux quantities of the related physical phenomenon. In the present numerical analysis, $\kappa-\varepsilon$ turbulent model proposed by Launder and Spalding (1972) was adopted. $\kappa-\varepsilon$ turbulent model introduces two additional equations namely turbulent kinetic energy (κ) and rate of dissipation (ε).

The equations for turbulent kinetic energy (κ) and rate of dissipation (ε) are given by;

$$div(\rho\overline{V}\kappa) = div\{(\mu+\mu_t)/\sigma_\kappa)grad\kappa)\}+G_\kappa-\rho\varepsilon \qquad (17)$$

$$div(\rho\overline{V}\varepsilon) = div\{(\mu+(\mu_t/\sigma_\varepsilon))grad\varepsilon)\}+C_{1\varepsilon}(\varepsilon/\kappa)G_\kappa+C_{2\varepsilon}\rho(\varepsilon^2/\kappa) \qquad (18)$$

In the above equations, G_κ represents the generation of turbulent kinetic energy due to mean velocity gradients, σ_κ and σ_ε are effective Prandtl numbers for turbulent kinetic energy and rate of dissipation respectively; $C_{1\varepsilon}$ and $C_{2\varepsilon}$ are constants and μ_t is the eddy viscosity and is modeled as

$$\mu_t=(\rho C_\mu\kappa^2)/\varepsilon, \qquad (19)$$

C_{μ} is a constant and its value is 0.09.

In the equations (17) and (18); $C_{1\varepsilon} = 1.44$; $C_{2\varepsilon} = 1.92$; $\sigma_{\kappa} = 1.0$ and $\sigma_{\varepsilon} = 1.3$.

Further information is available in Launder and Spalding (1972) and Fluent (2005) for turbulence modeling.

5.5.4 Boundary conditions

The governing equations of the fluid flow are non-linear and coupled partial differential equations, subjected to the following boundary conditions. At the tube inlet section, uniform axial velocity $V_{in,}$ temperature $T_{in,}$ turbulent intensity and hydraulic diameter (Fluent, 2005) have been specified. At the outlet section, the flow and temperature fields are assumed fully developed ((x/D) >10). Outflow boundary condition has been implemented for the outlet section. This boundary condition implies zero normal gradients for all flow variables except pressure. Only half of the tube was modeled due to the symmetry. On the upper wall of the tube, the no-slip boundary condition was imposed. The wall is subjected to a uniform heat flux. On the lower wall of the modeled domain, the symmetrical boundary condition was applied. Symmetric boundary condition implies; zero normal velocity at a symmetry plane and zero normal gradients of all flow variables at a symmetry plane. In the present analysis, the near wall treatment was based on enhanced wall functions (Fluent, 2005).

5.6 Numerical method

The computational fluid dynamics code Fluent was used for solving this problem. The system of governing equations (14) – (18) was solved by control volume approach. Control-volume technique converts the governing equations to a set of algebraic equations that can be solved numerically. The control volume approach employs the conservation statement or physical law represented by the entire governing equations over finite control volumes. First order upwind scheme was employed to discretize for the convection terms, diffusion terms and other quantities resulting from governing equations. Grid schemes used are staggered in which velocity components are evaluated at the center of control volume interfaces and all scalar quantities are evaluated in the center of control volume. Pressure and velocity were coupled using Semi Implicit Method for Pressure Linked Equations [SIMPLE] (Patankar, 1980). Fluent solves the linear systems resulting from discretization schemes using a point implicit (Gauss-Seidel) linear equation solver in conjunction with an algebraic multigrid method. During the iterative process, the residuals were carefully monitored. For all simulations performed in the present study, converged solutions were considered when the residuals resulting from iterative process for all governing equations (14) – (18) were lower than 10^{-6}.

5.7 Results and discussions

5.7.1 Validation of the present simulation

The tube has a diameter of 0.01 m and a length of 0.8 m. The fluid enters the tube with a constant inlet temperature T_{in} of 293 K and with uniform axial velocity V_{in}. The Reynolds number was varied from 10^4 to 10^5. In order to validate the computational model, the numerical results were compared with the theoretical data available for the conventional fluids. The Darcy friction factor given by Blasius is presented as Equation (20) from White (1991).

$$f = 4C_f = 4(0.0791\,\mathrm{Re}^{-1/4}) \tag{20}$$

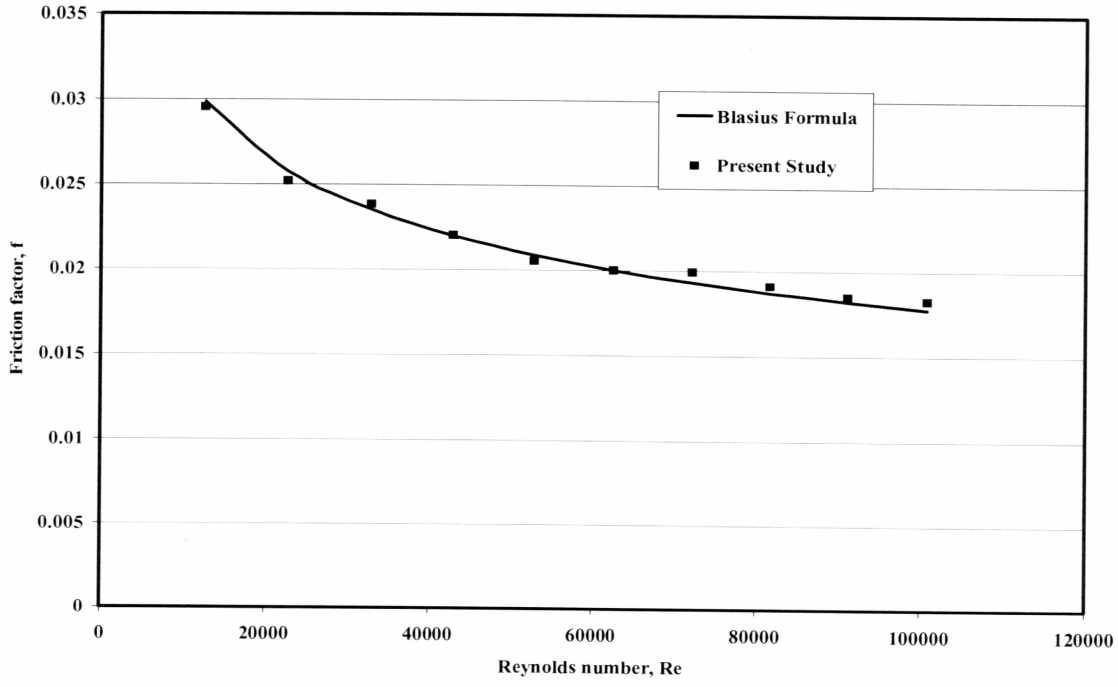

Figure 5.3 Comparison of Darcy friction factor by Blasius formula and computed values for EG/Water in turbulent regime.

Figure 5.3 displays the comparison of Darcy friction factor from Blasius formula and computed values from the present simulations. An excellent agreement is observed with maximum deviation and average deviation of computed values from theoretical equation being 3.2% and 1.9% respectively over the range of Reynolds numbers studied.

Next, the Nusselt number for the fully developed turbulent flow for EG/water is compared with the correlation given by Gnielinski (1976).

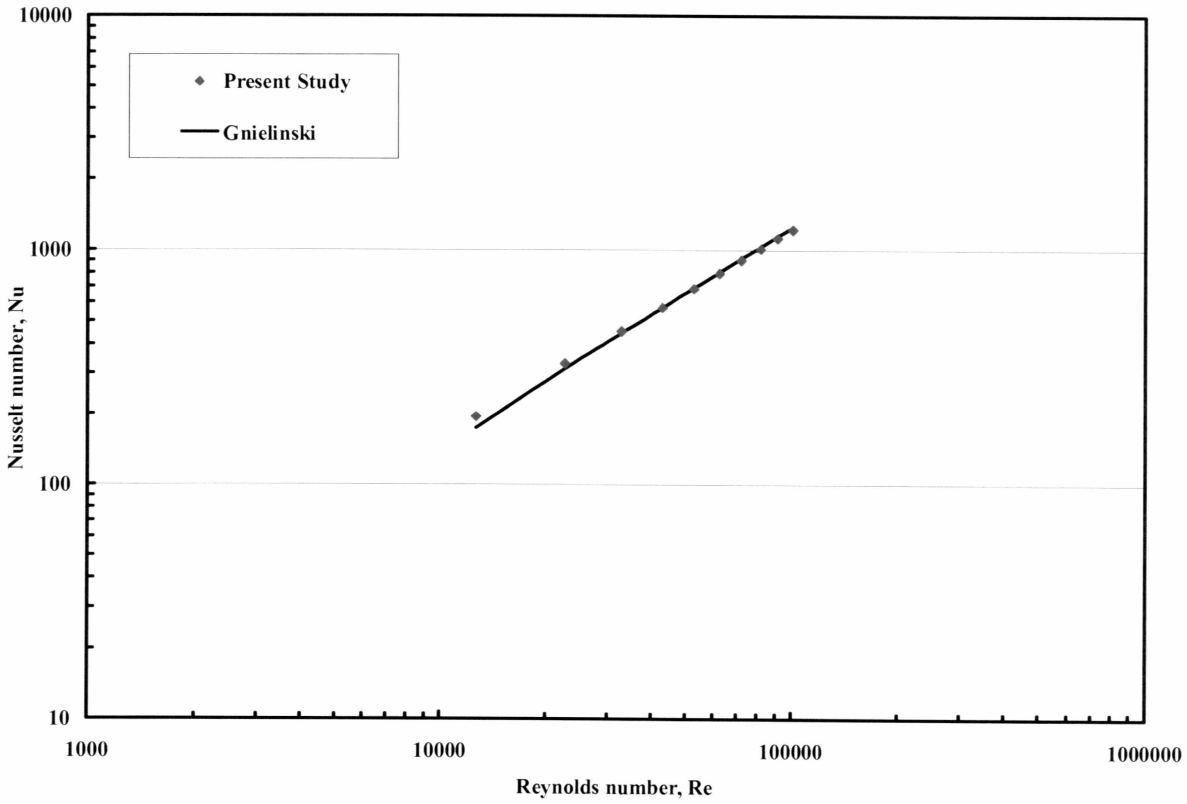

Figure 5.4 Comparison between the computed values of Nusselt numbers and the equation given by Gnielinski for EG/water.

Bejan (1993) recommends the equation given by Gnielinski, Equation (21) over the traditional Dittus – Boelter equation, because the errors are usually limited to about ± 10 %.

$$Nu = 0.012(Re^{0.87}-280)\, Pr^{0.4} \qquad (21)$$

For $1.5 \leq Pr \leq 500$, $3 X 10^3 \leq Re \leq 10^6$. Our simulations were all within this range. Figure 4 displays comparison of Nusselt numbers obtained from the present numerical analysis for fully developed flow with the equation given by Gnielinski for EG/water. The maximum deviation and average deviation of computed Nusselt number from the equation given by Gnielinski is 10.1% and 5.8% respectively.

5.7.2 Application of the model

After the above two comparisons and confirming that the computational model is generating correct results, nanofluids with varying concentrations were analyzed at various Reynolds numbers with applied constant heat flux q'' on the upper wall. A heat flux of 50 W/cm^2 was selected in our simulations because we wanted to compare our results with Maiga et al. (2006).

5.7.3 Effect of nanoparticle volume concentration on the Nusselt number

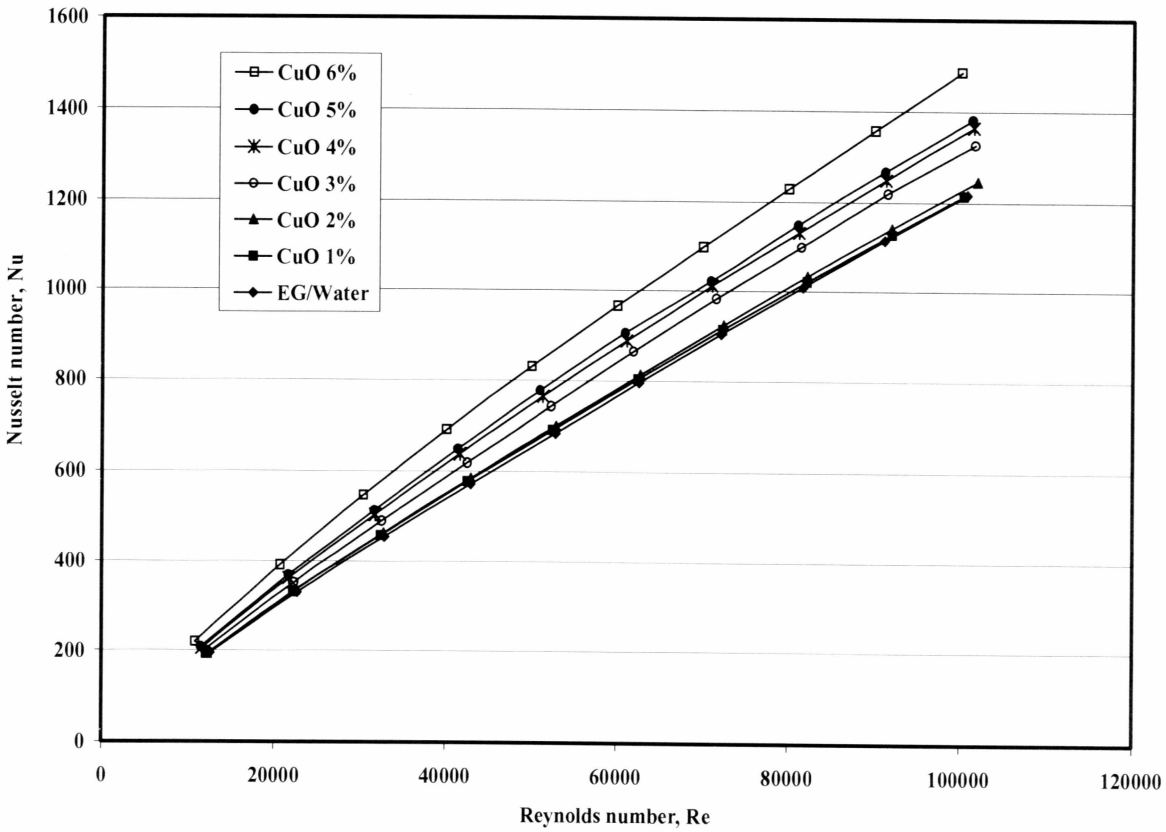

Figure 5.5 The influence of copper oxide nanoparticle volume concentration on the Nusselt number over a range of Reynolds numbers.

Figure 5.5 displays the influence of CuO nanoparticle volume concentration on the Nusselt number. As an example, the increase in the Nusselt number is about 1.35 times with 6% volume concentration of CuO nanoparticles over the base fluid EG/water at Reynolds number of 20000 and the increase in the Nusselt number is about 1.23 times at Reynolds number of 100000. The increase in the Nusselt number is due to the increase in Prandtl number at higher concentrations.

5.7.4 Comparison of computed Nusselt number with other correlations

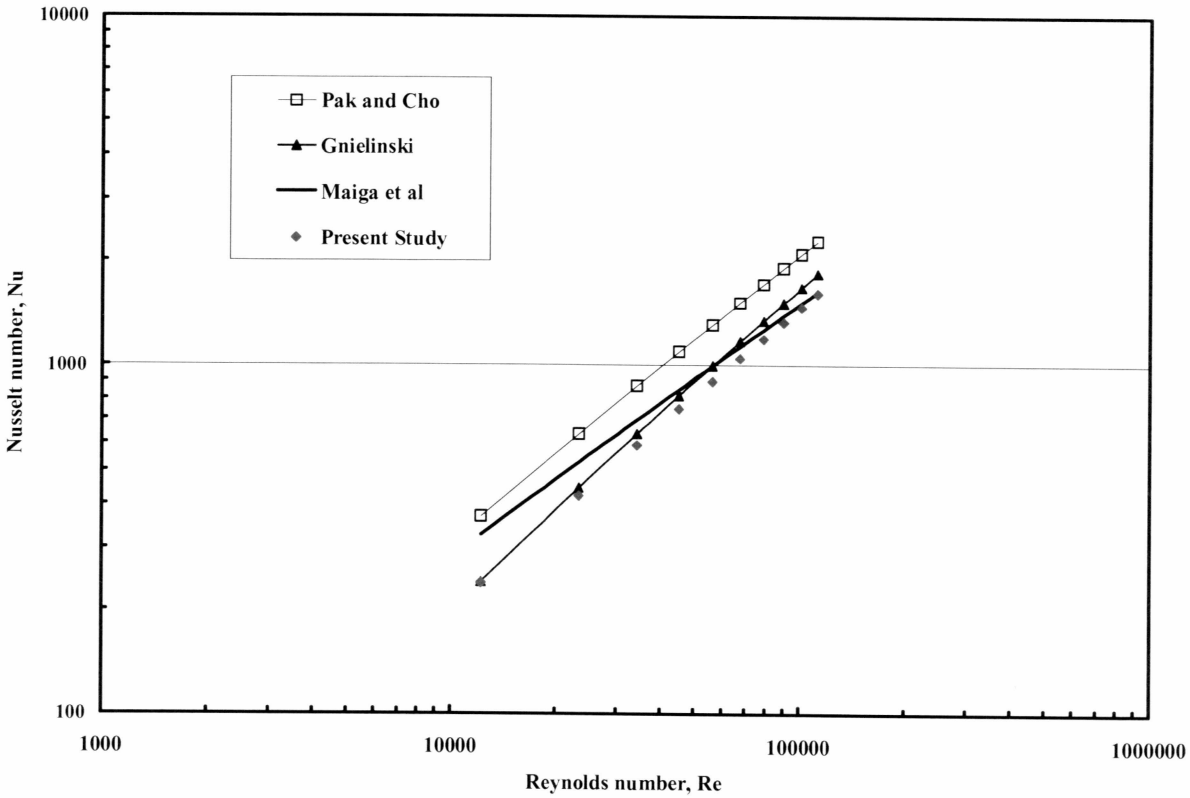

Figure 5.6 Comparison of Nusselt number for CuO (6%) with other correlations.

Figure 5.6 displays the comparison of computed Nusselt number from our simulations for a CuO 6% nanofluid with other correlations. As no experimental data is available for CuO 6% nanofluid, we compared our results with the correlation Equation (1) by Pak and Cho (1998). Pak and Cho developed the correlation from dilute concentration (0 – 3%) of Al_2O_3 and TiO_2 nanoparticles in water which have lower Prandtl numbers. The deviation between the present study and the Pak and Cho correlation is due to different nanofluids of higher concentration and higher Prandtl

number. Equation (2) by Maiga et al (2006) predicts higher Nusselt number at lower Reynolds number. This is because they have conducted their numerical computations using constant thermophysical properties evaluated at inlet temperature. However, in reality at lower Reynolds number, the fluid gets heated up and the bulk mean temperature of the fluid increases. This case was observed in our simulations. At higher bulk mean temperature the viscosity value becomes lower. As Prandtl number is directly proportional to viscosity it lowers the Prandtl number, which in turn lowers the Nusselt number which is evident from our simulation. However, at higher Reynolds numbers, the bulk mean temperature of the fluid does not change considerably; this does not affect the viscosity and the Prandtl number and hence there is a closer agreement between Maiga et al and the present simulation. The computed values of Nusselt number from the present simulation are in good agreement with the equation (21) developed by Gnielinski (1976). The maximum deviation and average deviation of computed values with equation by Gnielinski were 12% and 6.5%. A summary of the Prandtl number variation with Reynolds number is compiled in Figure 5.7.

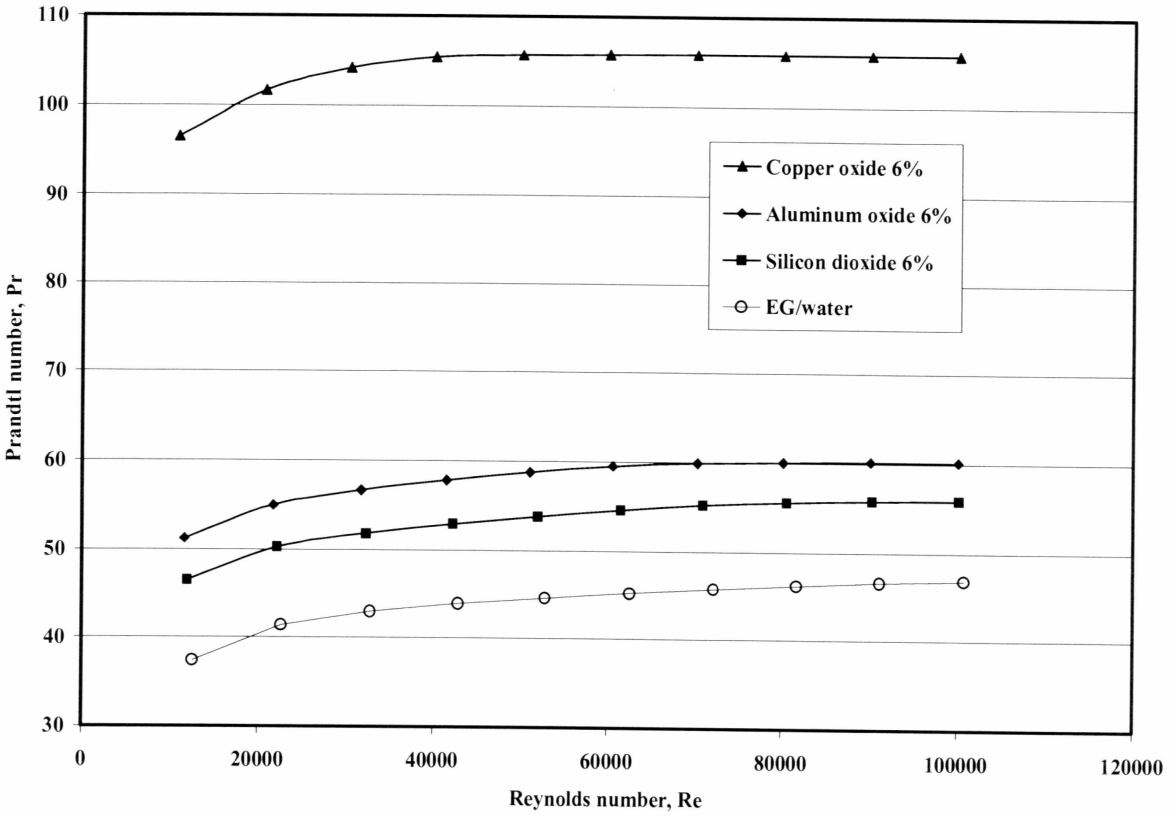

Figure 5.7 Variation of Prandtl number with Reynolds number in the present simulations for various nanofluids.

It can be concluded that for all nanofluids of same concentration Prandtl number is low at lower Reynolds numbers and high at higher Reynolds numbers. This is solely due to the bulk mean temperature variation. Similar trend was observed for all concentrations of CuO nanofluids.

5.7.5 Effect of nanoparticle volume concentration on the heat transfer coefficient

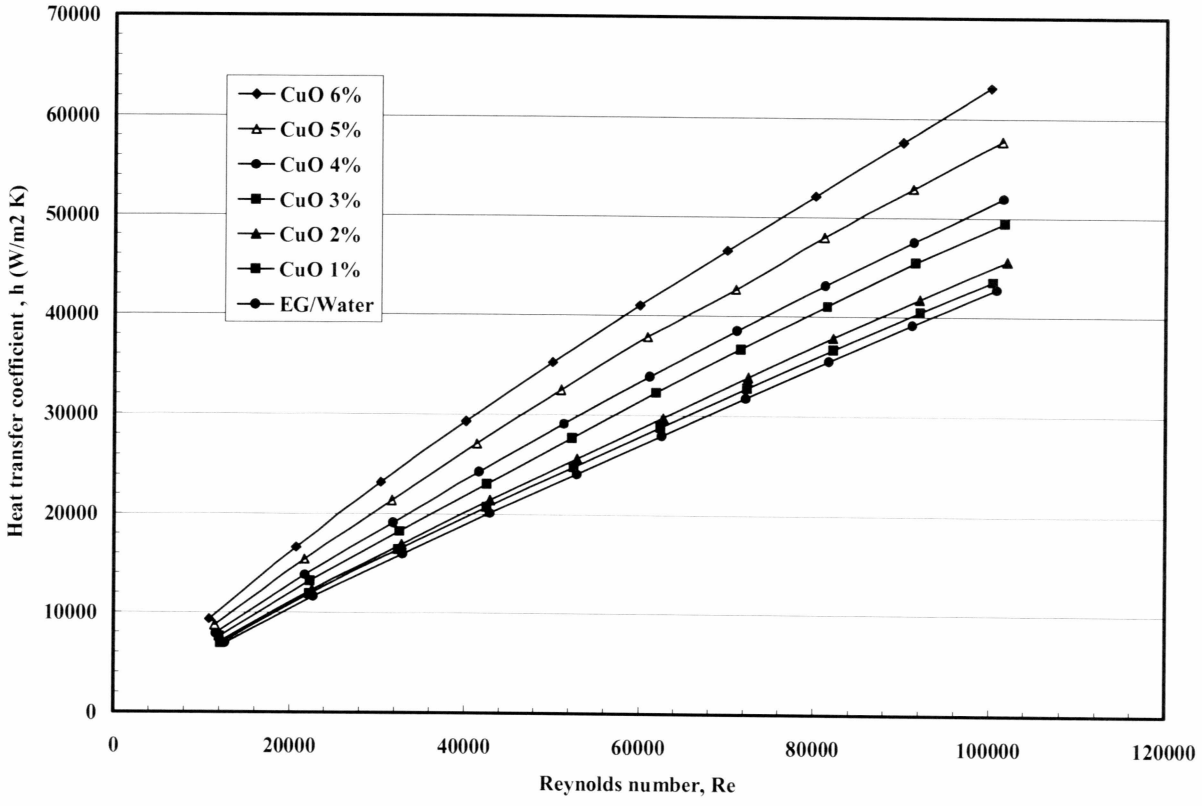

Figure 5.8 The influence of copper oxide nanoparticle volume concentration on the heat transfer coefficient over a range of Reynolds numbers.

Figure 5.8 displays the influence of CuO nanoparticle volume concentration on the heat transfer coefficient. For a 6% volume concentration, the increase in heat transfer coefficient is about 1.75 times over the base fluid at a Reynolds number of 20000 and is about 1.5 times at Reynolds number of 100000. At lower Reynolds number, the bulk mean temperature is higher making specific heat, thermal conductivity higher and

viscosity lower. Therefore a better heat transfer is achieved and hence the relative gain in heat transfer is higher at lower Reynolds number for a fixed concentration.

5.7.6 Comparison between different nanofluids of same volume concentration

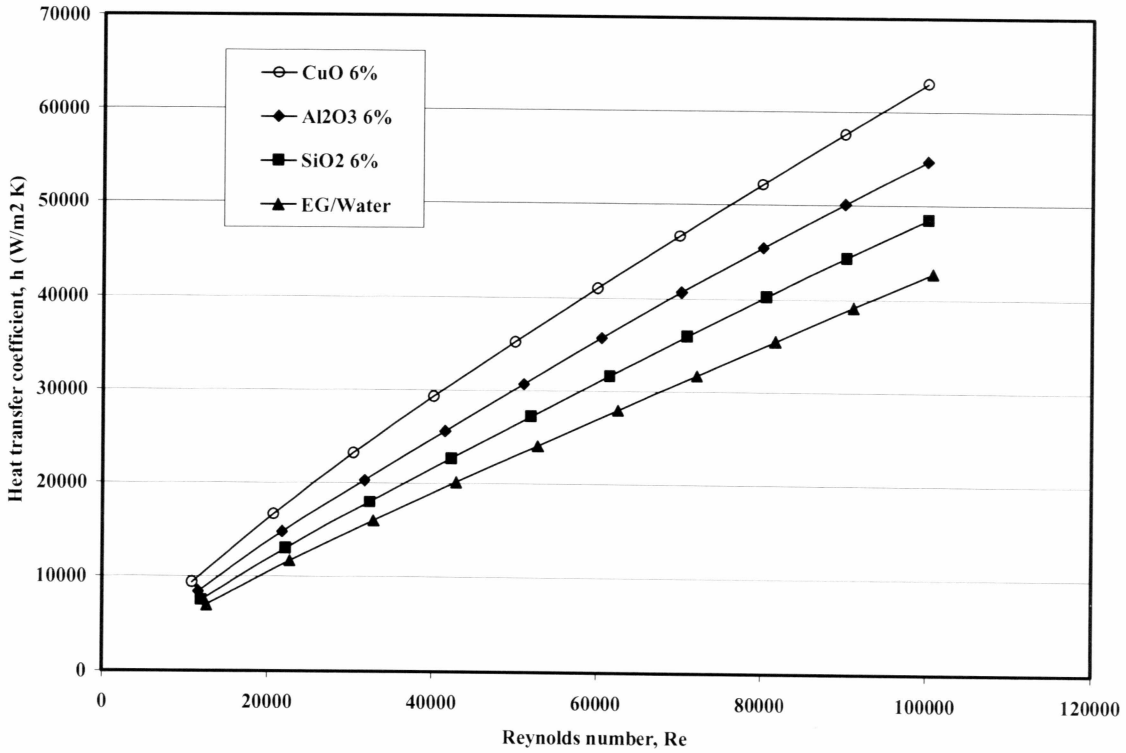

Figure 5.9 Comparison of heat transfer coefficient of different nanofluids over the base fluid EG/water.

Figure 5.9 displays the increase in heat transfer coefficient by various nanofluids over the base fluid for a fixed volume concentration of 6%. The increase in heat transfer coefficient is high for CuO nanofluids and is low for SiO_2 nanofluids. This is due to the higher Prandtl number and thermal conductivity of CuO nanofluids than others.

5.7.7 Effect of nanoparticle diameter on the Nusselt number

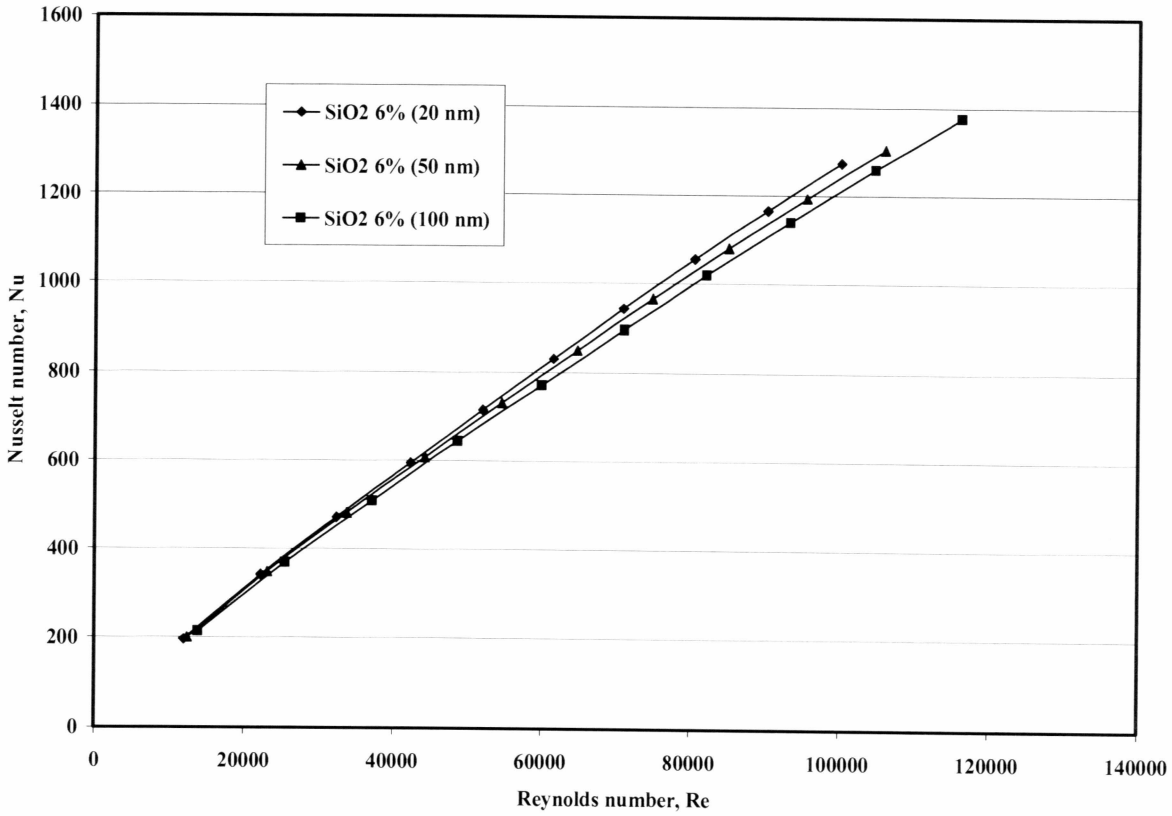

Figure 5.10 Effect of nanoparticle diameter on the Nusselt number for a 6% volume concentration of SiO2 nanofluids.

Figure 5.10 displays the effect of nanoparticle diameter on the Nusselt number for SiO_2 nanofluids of 6% volume concentration. The fluid containing 20 nm particle size have higher Nusselt numbers followed by 50 nm and 100 nm for same Reynolds number. This is because the viscosity values of 20 nm nanofluid are higher, followed by 50 nm and 100 nm. Higher the viscosity, higher the Prandtl number for same concentration of

SiO_2 nanofluids. Higher Prandtl number yields higher Nusselt number. Similar enhancement in Nusselt number with lower particle size was observed from the experiments conducted by Nguyen et al (2007). For the same volume concentration lower diameter particles provide large surface area of interaction with the fluid in exchanging heat

5.7.8 Effect of nanoparticle volume concentration on the wall shear stress

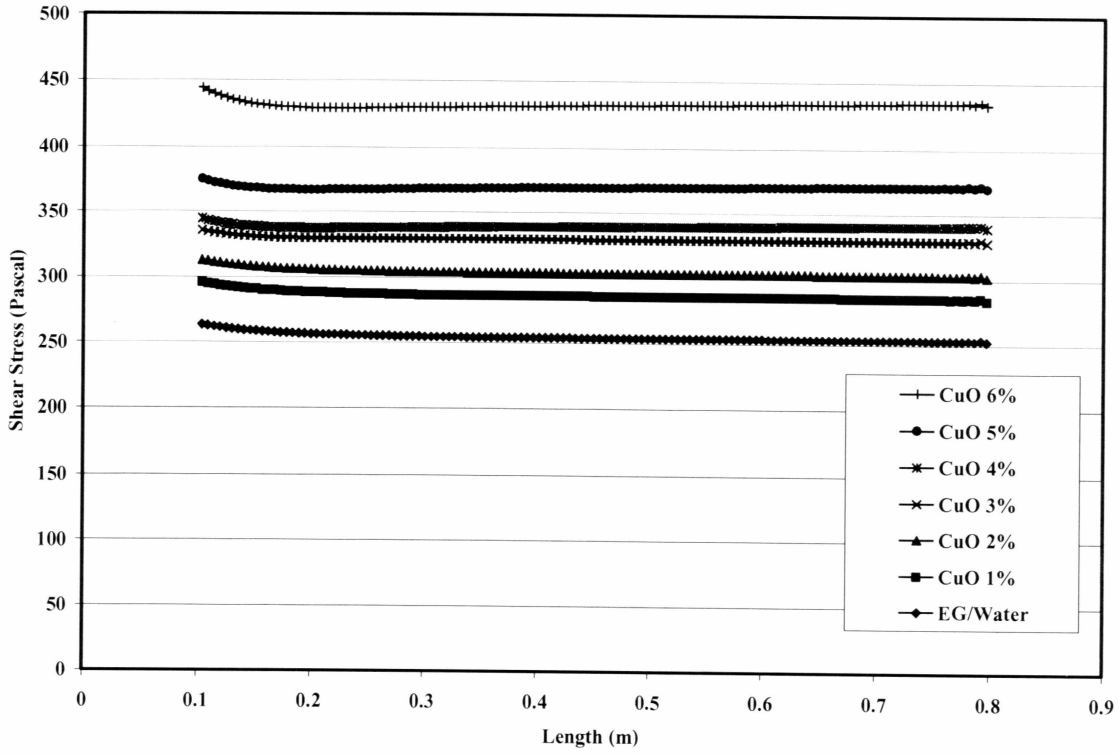

Figure 5.11 Effect of nanoparticle volume concentration on the wall shear stress for CuO nanofluids in the fully developed region.

From Figure 5.11, we observe that higher the concentration of the nanofluids, higher is the wall shear stress. Higher the shear stress, higher is the pumping power. Nanofluids

with higher volume concentration have higher heat transfer enhancement and also have higher pressure drop. Therefore, judicious decision should be taken when selecting a nanofluid that will balance the heat transfer enhancement and the pressure drop penalty.

5.8 Conclusions

Viscosity of nanofluids increases as the particle diameter decreases. New viscosity correlations for nanofluids as a function of volume concentration and temperature were presented. At a fixed Reynolds number of 20000 Nusselt number for 6% CuO nanofluids increases by 1.35 times over the base fluid. At a fixed Reynolds number of 20000 heat transfer coefficient for 6% CuO nanofluids increases by 1.75 times over the base fluid. Heat transfer coefficient of nanofluids increases with increase in the volume concentration of nanofluids and Reynolds number. Higher temperature operation of the nanofluids yields higher percentage increase in heat transfer rate. Prandtl number of nanofluids increases with decrease in the operating temperature, because the viscosity plays a dominant role. For the same concentration of CuO, Al_2O_3 and SiO_2 nanofluids, at a particular Reynolds number, CuO nanofluids have higher heat transfer performance followed by Al_2O_3 and SiO_2. Pressure loss increases with increase in the volume concentration of the nanofluids. Computed values of the Nusselt numbers are in good agreement with correlation given by Gnielinski. From our analysis we found that Gnielinski correlation can be used in determining the Nusselt number of nanofluids with $47 \leq Pr \leq 105$ and Reynolds number ranging 10^4-10^5 with concentration upto 6%.

5.9 Nomenclature

x	Distance from the inlet, m
L	Length of the tube, m
D	Diameter of the tube, m
T	Temperature, K
q''	Heat flux, W/m^2
V	Velocity, m/sec
c	Specific heat, J/kg.K
k	Thermal conductivity, W/m.K
h	Heat transfer coefficient, $(h = q''/T_w - T_{bm})$, $W/m^2.K$
Nu	Nusselt number, $Nu = (hD/K)$
Re	Reynolds number, $Re = (\rho VD/\mu)$
Pr	Prandtl number, $Pr = (\mu c/k)$
f	Friction factor
C_f	Skin friction coefficient

Greek Letters

ϕ	Volume concentration, %
ρ	Density, kg/m^3
μ	Viscosity, mPa.s

Subscripts

p	Nanoparticle
nf	Nanofluid

bf	Base fluid
in	Inlet
out	Outlet
w	Wall
bm	Bulk mean

5.10 Acknowledgements

Financial assistance from the Arctic Region Supercomputing Center (ARSC) and the Department of Mechanical Engineering at the University of Alaska Fairbanks is gratefully acknowledged.

5.11 References

Akbarinia, A., Behzadmer, A., 2007. Numerical study of laminar mixed convection of a nanofluid in horizontal curved tubes, Applied Thermal Engineering 27, 1327-1337.

ASHRAE Handbook Fundamentals., 2005. American Society of Heating, Refrigerating and Air-Conditioning Engineers Inc., Atlanta.

Batchelor, G.K., 1977, The effect of Brownian motion on the bulk stress in a suspension of spherical particles, Journal of Fluid Mechanics, 83, 97-117.

Bejan, A., 1993. Heat Transfer, John Wiley & Sons, New Jersey.

Brookfield Engineering., 1999. Brookfield LV DV-II+ Programmable Viscometer Manual No. M/97-164-D1000, Brookfield Engineering Laboratories Inc, Massachusetts.

Buongiorno, J., 2006. Convective transport in nanofluids, Journal of Heat Transfer 128, 240-250.

Choi, S., 1995., Enhancing thermal conductivity of fluids with nanoparticles, ASME Publications 66, 99-105.

Das, S., Putra, N., Thiesen, P., Roetzel, W., 2003. Temperature dependence of thermal conductivity enhancement for nanofluids, Journal of Heat Transfer 125, 567-574.

Dittus, F.W., Boelter, L.M.K., 1930. Heat transfer for automobile radiators of the tubular type, University of California Publications in Engineering 2, 443.

Eastman, J.A., Choi, S.U.S., Li, S., Yu, W., Thompson, L.J., 2001. Anomalously increased effective thermal conductivities of ethylene glycol-based nanofluids containing copper nanoparticles, Applied Physics Letters 78, 718-720.

Fluent 6.2 user guide, 2005. Fluent Inc, Lebanon, New Hampshire.

Gnielinski, V., 1976. New equations for heat and mass transfer in turbulent pipe and channel Flow, International Chemical Engineering 16, 359-367.

Hamilton, R. L., Crosser, O. K., 1962. Thermal conductivity of heterogeneous two-component system, I and EC Fundamentals 1,187-191.

Heris, S. Z., Esfahany, M. N., Etemad, G., 2006. Investigation of CuO/water nanofluid laminar convective heat transfer through a circular tube, Journal of Enhanced Heat Transfer 13, 279-289.

Kulkarni, D.P, Das, D.K, Patil, S.L., 2007. Effect of temperature on rheological properties of copper oxide nanoparticles dispersed in propylene glycol and water mixture, Journal of Nanoscience and Nanotechnology 7, 1-5.

Launder, B.E., Spalding, D.B., 1972. Mathematical models of turbulence, Academic Press, New York.

Maiga, S. B., Palm, S. J., Nguyen, C. T., Roy, G., Galanis, N., 2005. Heat transfer enhancement by using nanofluids in forced convection flows, International Journal of Heat and Fluid Flow 26, 530-546.

Maiga, S.B., Nguyen, C.T., Galanis, N., Roy., Mare, T., Coqueux, M., 2006. Heat transfer enhancement in turbulent tube flow using Al_2O_3 nanoparticle suspension, International Journal of Numerical Methods for Heat and Fluid Flow 16, 275-292.

McQuiston, F.C., Parker, J.D., Spitler, J.D., 2000. Heating Ventilating and Air conditioning, John Wiley & Sons Inc., New York.

Namburu, P.K., Kulkarni, D.P., Misra, D., Das, D.K., 2007. Viscosity of copper oxide nanoparticles dispersed in ethylene glycol and water mixture, Experimental Thermal and Fluid Science, In press.

Nguyen, C.T., Roy, G., Gauthier, C., Galanis, N, 2007. Heat transfer enhancement using Al_2O_3-water nanofluid for an electronic liquid cooling system, Applied Thermal Engineering 27, 1501-1506.

Pak, B. C., Cho, Y. I., 1998. Hydrodynamic and heat transfer study of dispersed fluids with submicron metallic oxide particles, Experimental Heat Transfer 11, 151-170.

Patankar, S. V., 1980. Numerical heat transfer and fluid flow, Hemisphere Publishing Corporation, New York.

Shih, T.M., 1984. Numerical Heat Transfer, Hemisphere Publishing Corporation, New York.

Xuan, Y., Li, Q., 2003. Investigation on convective heat transfer and flow features of nanofluids, Journal of Heat Transfer 125, 151-155.

Wang, X.Q., Mujumdar, A.S., 2007. Heat transfer characteristics of nanofluids: a review, International Journal of Thermal Sciences 46, 1-19.

White, F.M., 1991. Viscous Fluid Flow, McGraw Hill, New York.

Chapter Six

General Conclusions and Recommendations

A set of conclusions can be drawn from the studies described under Chapters 2 to 5.

6.1 Conclusions

1. Copper oxide nanofluids exhibit Newtonian behavior in an ethylene glycol and water mixture for concentrations varying from 0 to 6.12% with temperatures ranging from -35°C to 50°C.

2. The viscosity of CuO nanofluids increases when the volume concentration of nanoparticles increases. Viscosity of CuO, Al_2O_3 and SiO_2 nanofluids decreases exponentially with increase in temperature.

3. Three new empirical correlations were developed for nanofluids that related the viscosity with volume concentration and temperature.

4. Silicon dioxide nanofluids with ethylene glycol/water as base fluid exhibited non-Newtonian behavior at lower temperatures.

5. For the same particle volume concentration, as the particle diameter increases the viscosity of SiO_2 nanofluids decreases. This is physically quite realistic because for a given volume concentration, smaller diameter nanoparticles will be more in number and the total surface area of these smaller diameter nanoparticles will be more. Therefore, smaller diameter nanoparticles interact with the surrounding fluid over a greater surface area, thus increasing the viscosity.

6. The average Nusselt number for flow in a parallel plate duct as a function of Reynolds number and concentration has been numerically analyzed. This analysis for nanofluids show that Nusselt number increases with Reynolds number and also with particle volume concentration. However, the influence of Reynolds number is stronger. For example, Nusselt number increases from 73 to 277 for Reynolds number 100 to 2000 for a CuO particle concentration of 10% in water as the base fluid. This increase is less at a lower particle concentration.

7. For the laminar simulation, at a constant inlet velocity an increase in particle volume concentration results in much higher skin friction coefficient along the duct. The average skin friction coefficient of 10% CuO nanofluid in the fully developed region is about 4 times compared to water at a constant inlet velocity of 0.66 m/sec.

8. For the laminar developing flow simulation, the average skin friction and the pressure loss steadily increase with volume concentration of nanofluids. The pumping power increases substantially. Therefore, in order to receive the benefit of nanofluids for heat transfer under laminar developing flow regime, the nanofluids may be limited to lower concentrations or if the nanofluid is heated up substantially lowering the viscosity then the pressure loss can be reduced.

9. For the turbulent flow simulation of nanofluids through a circular tube, at a fixed Reynolds number of 20000, Nusselt number for 6% CuO nanofluids in ethylene glycol and water mixture increases by 1.35 times over the base fluid. At a fixed Reynolds number of 20000, the heat transfer coefficient for 6% CuO nanofluids increases by 1.75

times over the base fluid. In general, the heat transfer coefficient of nanofluids increases with increase in the volume concentration of nanoparticles and Reynolds number.

10. For the same volume concentration of CuO, Al_2O_3 and SiO_2 nanofluids, at a particular Reynolds number, CuO nanofluids have higher heat transfer performance followed by Al_2O_3 and SiO_2.

11. For the same kind of nanofluids, those containing smaller diameter nanoparticles have higher heat transfer coefficient than the nanofluids containing larger diameter nanoparticles.

12. Nanofluids with higher volume concentration of nanoparticles have higher heat transfer enhancement and also have higher pressure drop. Therefore, judicious decision should be taken when selecting a nanofluid concentration that will balance the heat transfer enhancement and the pressure loss penalty.

6.2 Recommendations

1. Currently researchers are using the Hamilton and Crosser's correlation for thermal conductivity which is fairly old and does not take temperature dependence into account exclusively. Therefore, experimental investigation of the thermal conductivity of different nanofluids and development of appropriate correlations are recommended. The effect of all the thermophysical properties on the Prandtl number should be evaluated.

2. In this thesis, we have simulated nanofluid as a heating medium. However, they can also be used for cooling purpose replacing chilled water and glycol solutions. Therefore, a numerical analysis with outward heat flux as the boundary condition from the tube should be performed to explore the benefits of nanofluid in cooling applications.

Appendix

The following table provides the information about the cost of various nanofluids used in the present study. All the nanofluids as dispersions were purchased from Alpha Aesar Inc.

Table A 1. Cost of various nanofluids.

Type of nanofluid	Size	Price
Aluminum oxide in water colloidal dispersion	500g	$67.20
Copper oxide in water colloidal dispersion	500g	$321.00
Silicon dioxide in water colloidal dispersion	500g	$40.00